REVIEW

A Review of the Interactions between Tropical Cyclones and Environmental Vertical Wind Shear

ROSIMAR RIOS-BERRIOS,[a] PETER M. FINOCCHIO,[b] JOSHUA J. ALLAND,[c,d] XIAOMIN CHEN,[e,f] MICHAEL S. FISCHER,[g,f] STEPHANIE N. STEVENSON,[d] AND DANDAN TAO[h]

[a] *National Center for Atmospheric Research, Boulder, Colorado*
[b] *Naval Research Laboratory, Monterey, California*
[c] *University Corporation for Atmospheric Research, Boulder, Colorado*
[d] *NOAA/National Hurricane Center, Miami, Florida*
[e] *Department of Atmospheric and Earth Science, University of Alabama in Huntsville, Huntsville, Alabama*
[f] *NOAA/OAR/Atlantic Oceanographic and Meteorological Laboratory, Miami, Florida*
[g] *Cooperative Institute For Marine And Atmospheric Studies, University of Miami, Miami, Florida*
[h] *Geophysical Institute, University of Bergen, Bergen, Norway*

(Manuscript received 14 February 2023, in final form 14 August 2023, accepted 24 October 2023)

ABSTRACT: Tropical cyclone (TC) structure and intensity are strongly modulated by interactions with deep-layer vertical wind shear (VWS)—the vector difference between horizontal winds at 200 and 850 hPa. This paper presents a comprehensive review of more than a century of research on TC–VWS interactions. The literature broadly agrees that a TC vortex becomes vertically tilted, precipitation organizes into a wavenumber-1 asymmetric pattern, and thermal and kinematic asymmetries emerge when a TC encounters an environmental sheared flow. However, these responses depend on other factors, including the magnitude and direction of horizontal winds at other vertical levels between 200 and 850 hPa, the amount and location of dry environmental air, and the underlying sea surface temperature. While early studies investigated how VWS weakens TCs, an emerging line of research has focused on understanding how TCs intensify under moderate and strong VWS (i.e., shear magnitudes greater than 5 m s^{-1}). Modeling and observational studies have identified four pathways to intensification: vortex tilt reduction, vortex reformation, axisymmetrization of precipitation, and outflow blocking. These pathways may not be uniquely different because convection and vortex asymmetries are strongly coupled to each other. In addition to discussing these topics, this review presents open questions and recommendations for future research on TC–VWS interactions.

KEYWORDS: Dynamics; Wind shear; Tropical cyclones; Thermodynamics

1. Background

Meteorologists started to notice that the vertical profile of horizontal winds influences tropical cyclone (TC) formation and intensification even before the advent of weather satellites. Based on observations of different types of clouds, Weightman (1919) argued that deep easterlies through the troposphere were conducive for the formation of the 1919 West India TC. This argument was also supported by Riehl and Shafer (1944), who performed an analysis of balloon-based wind charts at the Institute of Tropical Meteorology in Puerto Rico. They found that deep easterlies to the north of tropical disturbances were most favorable for TC development, but that a vertical profile with easterlies at the surface and westerlies at 14 000 ft (approximately 4.3 km) "prevented development of strong rotating vortices" in the North Atlantic. Fifteen years later, Ramage (1959) analyzed balloon-based wind charts and found that large changes in the horizontal winds with height also prevented TC development over the South China Sea and the Bay of Bengal. These early studies using cloud motions and sparse sounding observations provided some of the first evidence that TCs are most likely to form where the horizontal winds have small variations with height.

As aircraft and satellite observations became available later in the twentieth century, more detailed studies were conducted to explore the effects of the wind profile on TC development and intensification. Simpson and Riehl (1958) introduced the concept of "ventilation," where dry air is imported from the environment into the TC inner core by the vertically sheared flow. López (1968) combined flight-level observations with satellite data to compare a disturbance that developed into Hurricane Carla (1961) with a disturbance that did not develop into

Corresponding author: Rosimar Rios-Berrios, rberrios@ucar.edu

DOI: 10.1175/JAS-D-23-0022.1

a TC. This comparison showed that the disturbance that did not evolve into a TC was embedded in an environment with stronger vertical wind shear (VWS) than the disturbance that later became Hurricane Carla (López 1968). This result was generalized with composites of satellite observations of upper- and lower-tropospheric winds for developing and nondeveloping disturbances around the world (Gray 1968). These composites showed that TC development occurred where the VWS was "a minimum or zero"—a finding that was later supported by the composites of McBride and Zehr (1981). The composite approach was also employed by Merrill (1988), except this study compared intensifying and nonintensifying TCs. Consistent with previous studies, intensifying TCs were characterized by weaker VWS than nonintensifying TCs.

Due to limited wind observations within the middle troposphere, Gray (1968) and others defined VWS as the wind vector difference between 200 and 850 hPa. The shear calculated between these two pressure levels is commonly referred to as the "deep-layer" VWS. In calculating the deep-layer VWS around a TC, early studies such as Gray (1968) considered the full vector difference—that is, including both the environment and the TC winds—between the observed winds at these two levels. Gray (1968) and others did not account for the VWS that is induced by the TC itself given that the strongest winds in TCs are located in the lower troposphere and that the winds turn from cyclonic to anticyclonic with height. Subsequent studies developed various methods to estimate the VWS primarily contributed by the environmental winds (e.g., Kurihara et al. 1993; DeMaria and Kaplan 1994; Galarneau and Davis 2013; Wang et al. 2015). These methods have been reevaluated and challenged over the past decades due to limitations and uncertainties in their estimations of *environmental* VWS (Velden and Sears 2014; Ryglicki et al. 2020; Dai et al. 2021; Ryglicki et al. 2021).

The strong influence of deep-layer VWS magnitude on TC intensity motivated the inclusion of this variable in statistical models for intensity prediction. One of the first models to include VWS was the Statistical Hurricane Intensity Prediction Scheme (SHIPS) model (DeMaria and Kaplan 1994), in which deep-layer VWS magnitude was ranked as the second most important predictor of TC intensity (only behind the maximum potential intensity). The deep-layer VWS is a key predictor in more recent versions of the SHIPS model and other statistical models for intensity prediction (DeMaria and Kaplan 1999; Emanuel et al. 2004; DeMaria et al. 2005). New shear-related predictors quantifying shear in shallower layers have also been incorporated into these models. Deep-layer VWS is routinely estimated from real-time satellite products (see, e.g., https://tropic.ssec.wisc.edu/), and it is one of the key variables routinely examined by hurricane forecasters.

The important relationship between deep-layer VWS and TC intensity has inspired a plethora of studies since the 1990s aimed at understanding the effects of VWS on TC formation, intensity, and structure. Jones (1995) and DeMaria (1996) were among the first studies to show that a TC vortex is tilted in the presence of VWS. These studies, which relied on low-complexity computer models of TC-like vortices, also found that the tilted vortex resulted in asymmetric patterns of upward and downward motions around the TC center. Several years later, observational studies confirmed these findings by documenting that TCs under VWS exhibited enhanced precipitation in their downshear quadrants, and suppressed precipitation in their upshear quadrants (Black et al. 2002; Corbosiero and Molinari 2002; Chen et al. 2006; Cecil 2007; Hence and Houze 2011; Reasor et al. 2013; DeHart et al. 2014). Detailed observations, including those taken during field campaigns, enabled detailed case studies (Molinari et al. 2006; Shelton and Molinari 2009; Molinari and Vollaro 2010; Stevenson et al. 2014; Bukunt and Barnes 2015; Rogers et al. 2015; Zawislak et al. 2016; Rogers et al. 2016; Nguyen et al. 2017; Ryglicki et al. 2021; Wadler et al. 2021b; Alvey et al. 2022) and multicase composite analyses (Rogers et al. 2013; Reasor et al. 2013; DeHart et al. 2014; Wadler et al. 2018; Fischer et al. 2022) of TC–VWS interactions. The recent theoretical and modeling developments of the concept of "ventilation," which was originally coined by Simpson and Riehl (1958), has led to further advancement in our understanding of the thermodynamic impacts of VWS on TC structure and intensity (Tang and Emanuel 2010; Riemer et al. 2010). While much of the focus of early work on TC–VWS interactions centered around how TCs weakened under the influence of VWS, a new line of research has emerged focusing on how certain TCs can intensify while interacting with moderate to strong shear.

This review article provides a comprehensive summary of the scientific literature on TC–VWS[1] interactions and their effects on TC structure and intensity changes. While other review articles have broadly summarized the existing knowledge about TCs (Emanuel 2003; Wang and Wu 2004; Smith and Montgomery 2015; Montgomery and Smith 2017; Emanuel 2018), those articles only provide brief discussions about TC–VWS interactions owing to their broad scope. Their limited discussions together with a more than doubling of peer-reviewed manuscripts on the topic during the last decade motivated this synthesis solely focused on TC–VWS interactions. Recent advances in modeling and analysis techniques, including artificial intelligence/machine learning, and the proliferation of novel observing platforms offer several new avenues for research on sheared TCs. By summarizing the rapidly growing body of research and identifying key knowledge gaps, this review can serve as a starting point for future research utilizing new tools, techniques, and datasets to better understand and predict sheared TCs.

We begin our review by discussing how VWS, both by itself and in combination with other environmental factors, influences TC structure and intensity (sections 2 and 3). This discussion sets the stage for a review of knowledge about how TCs can intensify—sometimes rapidly—under moderate to strong VWS (section 4). The intricate multiscale nature of processes associated with TC–VWS interactions presents unique predictability challenges, and we summarize the work on this topic in section 5. Last, we present our conclusions, open questions, and recommendations for future research in section 6.

[1] Hereafter, the acronym "VWS" will refer to deep-layer (200–850 hPa) environmental shear of the horizontal wind.

2. Effects of VWS on TC structure and intensity

A central focus of TC research is understanding how a storm responds to both external and internal factors (Emanuel 2018). The literature on TC–VWS interactions offers plenty of evidence that VWS is one of the most influential external factors of TC structure. This section will describe the main effects of VWS on TC structure and how those effects can modulate TC intensity changes under environmental sheared flow.

a. Vortex tilt

If a TC is represented by a column of potential vorticity, a vertically sheared flow will differentially advect the vortex column. This process results in a vertically tilted vortex as illustrated in Fig. 1. The earliest work on TC vortex tilt focused on dry dynamics. Jones (1995) was among the first to document in detail the dynamics of vortex tilt using dry, adiabatic, and nonhydrostatic models. Her seminal work showed that vortex tilt magnitude is largely dependent on VWS magnitude and on properties of the TC vortex (e.g., size, strength). The dynamics of vortex tilt evolution have been described by two different paradigms: 1) potential vorticity anomalies and 2) vortex Rossby waves.

The first paradigm relies on "potential vorticity" thinking to describe how the winds associated with the tilted vortex modulate both the direction and magnitude of vortex tilt (Jones 1995, 2000a,b). In this view, the winds associated with an upper-tropospheric vorticity anomaly due to the tilted vortex can advect the lower-tropospheric vorticity anomaly and vice versa (Jones 1995). Provided the environmental vertical wind shear is not strong enough to irreversibly shear apart the TC (e.g., Smith et al. 2000; Reasor et al. 2004), the upper and lower portions of a tilted vortex will begin to corotate, or precess, cyclonically about one another (Jones 1995; Wang and Holland 1996; Jones 2000a; Reasor and Montgomery 2001; Reasor et al. 2004). In a quiescent environment, the upper and lower portions of the tilted TC vortex may continue to orbit around one another multiple times; however, in the presence of a sheared background flow, dry idealized modeling studies have discovered a preferred tilt orientation along—and to the left of—the VWS vector (Jones 1995; Wang and Holland 1996; Reasor et al. 2004). When the vortex tilt is directed downshear left, the projection of the cyclonic flow associated with the storm's lower-tropospheric circulation onto the displaced mid–upper-tropospheric circulation acts to oppose the environmental vertical wind shear, which can halt the cyclonic precession of the vortex. This process can also lead to vortex tilt reduction, which will be discussed in detail in section 4a.

The second paradigm describes vortex tilt evolution as being governed by vortex Rossby waves (Reasor and Montgomery 2001; Schecter et al. 2002; Schecter and Montgomery 2003; Reasor et al. 2004; Reasor and Montgomery 2015). These waves, which are excited by a tilted vortex under VWS, are analogous to midlatitude Rossby waves except their restoring mechanism is the radial vorticity gradient of the TC vortex. By examining a tilted quasigeostrophic vortex in a dry model, Reasor and Montgomery (2001) found the evolution of vortex tilt was consistent with the projection of the tilted vortex onto a near-discrete VRW, or "quasi mode," which is similar to an edge wave propagating on a Rankine vortex. In this paradigm, the evolution of vortex tilt is largely described by the azimuthal propagation and, as will be discussed in more detail in section 4a, inviscid damping of the discrete vortex Rossby waves that are excited by shear.

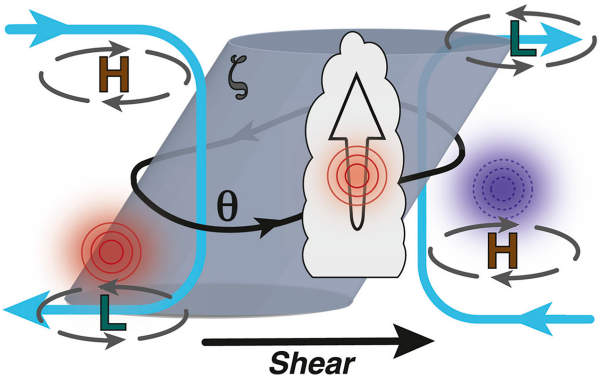

FIG. 1. Summary schematic of the kinematic and thermodynamic structure of Hurricane Rita (2005). The gray cylinder represents the vortex tower of the eyewall, which is tilted by the environmental wind shear (black vector). Green "L" symbols and vectors denote cyclonic low pressure anomalies, and brown "H" symbols denote anticyclonic high pressure anomalies. Thermal anomalies are denoted by blue (cold) and red (warm) circles and shading associated with slanted isentropic surfaces. Cyan arrows show the modified secondary circulation. The thick black contour denotes a representative potential temperature surface, with arrows illustrating the cyclonic vortex flow around the eyewall. In the downshear-right quadrant, air parcels move cyclonically downstream and adiabatically upward along the potential temperature surface resulting in individual convective motions denoted by the cumulus cloud and upward arrow. A warm anomaly is shown in the convective cloud to denote the release of latent heat associated with the buoyant updraft. From Fig. 15 in Boehm and Bell (2021).

In a balanced framework, tilted TC vortices are associated with thermal and convective asymmetries (Jones 1995; DeMaria 1996; Jones 2000a; Xu and Wang 2013; Boehm and Bell 2021), as reflected by the schematic in Fig. 1. More specifically, a cold anomaly is found in the downtilt region of the storm, whereas a warm anomaly is located within the uptilt portion (Jones 2000a). Observations of tilted, mature TCs corroborate this balanced thermal state (Reasor and Eastin 2012; Boehm and Bell 2021). The structure of a tilted TC vortex also varies vertically, as the direction of vortex tilt and the corresponding vorticity and temperature anomalies rotate anticyclonically with height (Jones 2000a; Reasor and Eastin 2012; Boehm and Bell 2021). These tilt-induced thermal asymmetries impact the TC convective structure, as will be discussed in more detail in the following subsection. As air travels cyclonically around the TC vortex, adiabatic ascent is promoted along upward-slanted isentropes located to the right-of-tilt direction; however, observations indicate convectively driven diabatic heating maximizes in the downtilt portion of the inner core (Reasor and Eastin 2012; Reasor et al. 2013; Boehm and Bell 2021). The location of peak ascent may be influenced by other factors, such as diabatic

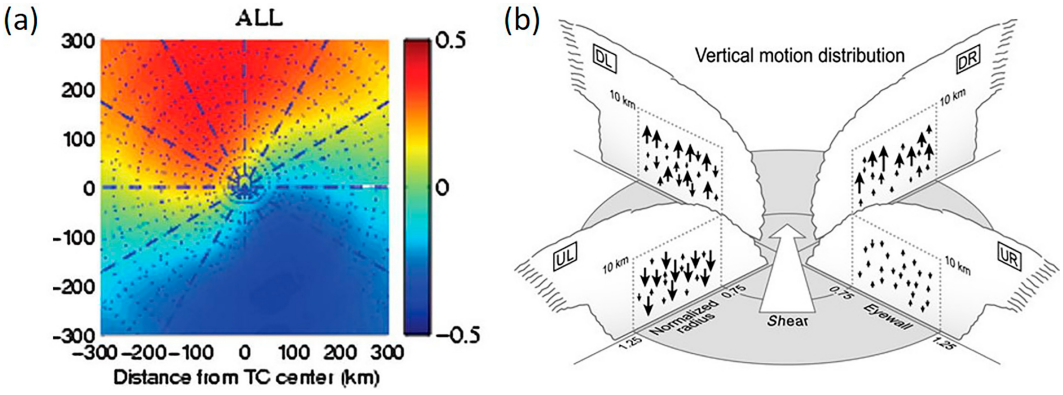

FIG. 2. (a) Fraction of the wavenumber-1 asymmetry of rainfall rates normalized by the azimuthal mean value (shading) relative to the 200–850 hPa environmental VWS, with the shear vector pointing to the top (adapted from Fig. 4a in Chen et al. 2006). (b) Schematic of the vertical motion distribution in a sheared environment. The environmental shear vector is denoted by the white arrow, and quadrants are labeled according to their direction relative to the shear vector (DR: downshear right; DL: downshear left; UL: upshear left; UR: upshear right) [adapted from Fig. 15a in DeHart et al. (2014)].

lifting, microphysical processes, and frictional convergence (e.g., Frank and Ritchie 2001; Didlake and Kumjian 2018; Feng and Bell 2019; Laurencin et al. 2020; Schecter 2022). Additionally, the magnitude of the asymmetric ascent depends on the TC vortex strength and VWS magnitude, among other factors (Jones 2000a; Xu and Wang 2013; Finocchio and Rios-Berrios 2021).

If a TC is not strong enough to be characterized by a column of potential vorticity, the effects of VWS on the vortex structure differ from those discussed above. Consider, for example, a weak tropical storm. The vortex structure is most likely shallow in comparison to the vortex of a major hurricane (Fischer et al. 2022). The extent to which VWS can "tilt" such a shallow vortex is unclear from the existing literature. Instead, idealized numerical simulations and airborne radar observations suggest that tropical storms and other weak TCs under VWS exhibit displaced centers of circulations in the middle and lower troposphere (Nugent and Rios-Berrios 2018; Rios-Berrios et al. 2018; Ryglicki et al. 2018b; Rogers et al. 2020; Schecter and Menelaou 2020; X. Chen et al. 2021; Schecter 2022; Fischer et al. 2022). Convective anomalies and their associated outflow coevolve with the tilted vortex, as demonstrated in satellite observations (Ryglicki et al. 2018a, 2019) and idealized simulations (Rios-Berrios et al. 2018; Ryglicki et al. 2018b; Schecter 2022). The corresponding thermodynamic response includes both warm anomalies above the surface circulation and cool anomalies below the middle-tropospheric circulation (Tao and Zhang 2019). Vertical motions respond more strongly to buoyant accelerations underneath the midtropospheric vortex (Ryglicki et al. 2018b) and to frictional convergence (Schecter 2020, 2022) than to the adiabatic ascent and descent induced by the temperature anomalies. Consequently, the evolution of vortex misalignment in weak vortices is largely governed by the influences of diabatic processes (Kwon and Frank 2008; Hogsett and Stewart 2014; Nguyen and Molinari 2015; Rios-Berrios et al. 2018; Ryglicki et al. 2018b; Tao and Zhang 2019; Rogers et al. 2020; Schecter and Menelaou 2020; Schecter 2022; Stone et al. 2023). However, the literature on vortex tilt of weak TCs is limited, and this is an area of much needed research.

b. *Asymmetric precipitation*

The asymmetric pattern of vertical motions that results from VWS tilting a mature TC vortex influences the distribution of precipitation around the storm center. Moderate to strong VWS (i.e., magnitudes exceeding 2.5 m s^{-1}) can produce a distinct wavenumber-1 precipitation asymmetry, with most precipitation occurring downshear and the maximum precipitation in the inner core located downshear left (Fig. 2a). This relationship is consistent across many observational (e.g., Corbosiero and Molinari 2002; Chen et al. 2006; Wingo and Cecil 2010; Pei and Jiang 2018; Stevenson et al. 2016) and modeling (e.g., Rogers et al. 2003; Braun et al. 2006) studies using a variety of metrics for measuring convective intensity. The downshear-left quadrant corresponds to the previously described preferential tilt orientation. Convective initiation is favored within the downshear-right quadrant (Fig. 2b), but the inner-core precipitation maximum occurs downwind in the downshear-left quadrant due to a combination of strong ascent and azimuthal advection of hydrometeors (Hence and Houze 2011; Reasor et al. 2013; DeHart et al. 2014). In the outer region of mature TCs known to contain the outer rainbands, convection is maximized downshear right due to the adiabatic ascent induced by the vortex tilt (Corbosiero and Molinari 2002; Stevenson et al. 2016). This region exhibits a persistent and nearly stationary region of precipitation, known as the stationary band complex (Willoughby et al. 1984; Riemer 2016).

Asymmetric convection within the downshear-left quadrant of weak to moderately sheared TCs provides a focal point for the formation of concentric eyewalls that can lead to eyewall replacement cycles (Wang and Tan 2022). Using airborne Doppler radar observations in Hurricane Earl (2010), Didlake et al. (2018) showed that a descending airstream, originating in the asymmetric stratiform precipitation, enhanced the boundary

layer convergence outside the eyewall and eventually led to the formation of a secondary eyewall.

While shear is frequently the dominant factor in causing azimuthal precipitation asymmetries in TCs (Chen et al. 2006), Stevenson et al. (2016) found that rainfall asymmetries were more closely tied to the storm motion vector for fast-moving TCs. Those TCs exhibited an upshear lightning maximum, suggesting that shear alone could not explain their convective asymmetries. Other factors—including frictional convergence, orographic lifting, and the TC circulation—also contribute to TC rainfall production and organization (Lonfat et al. 2004, 2007; Lu et al. 2018). Additional research is needed to understand the relative importance of each factor.

c. *Ventilation*

VWS can also impact the thermodynamic and convective TC structure through ventilation—or simply, the transport of low-equivalent potential temperature (θ_e) air into the TC inner core. Ventilation occurs through either vertical fluxes of low-θ_e air in downdrafts, radial fluxes of low-θ_e air from the environment, or a combination of both mechanisms. The literature has traditionally labeled ventilation pathways based on their vertical position (i.e., low-level, midlevel, and upper-level ventilation). However, in this review, we adopt the terms downdraft and radial ventilation to establish a clear relationship to the physical mechanism responsible for transporting low-θ_e air into the inner TC circulation (Alland et al. 2021a,b). We recognize that these processes are not fully independent of each other and they can both coexist at a given time (Riemer et al. 2010).

1) DOWNDRAFT VENTILATION

Downdraft ventilation refers to downward transport of low-θ_e air. Riemer et al. (2010) identified downdraft ventilation in low to midlevels as being associated with the shear-induced, wavenumber-1 precipitation asymmetry and the stationary band complex described in Willoughby et al. (1984). As precipitation from convection downshear is transported cyclonically left of shear and upshear, it evaporates into the unsaturated air below to develop downdrafts. The evaporatively cooled downdraft air within the subcloud layer is generally transported radially outward upshear, which can limit the areal extent of convection there, and radially inward right of shear (Riemer et al. 2010, 2013; Shu et al. 2014; Molinari et al. 2013; Alland et al. 2021a; see Fig. 4a). The magnitude of downdraft ventilation and the extent to which it limits TC development generally increases as the magnitude of VWS increases, as shown in Fig. 3.

The extent to which downdraft ventilation affects TC structure and intensity is sensitive to the ability of surface fluxes to recover the θ_e. The term recovery in this context refers to the process by which enthalpy fluxes from the sea surface increase the θ_e of evaporatively cooled downdraft air in the subcloud layer back toward the local saturation value. In many cases, air parcels are unable to fully recover from the effects of downdraft ventilation (e.g., Riemer et al. 2010), which makes the boundary layer upshear dynamically (i.e., radial outflow) and thermodynamically (i.e., lower θ_e) less favorable for deep convection. As such, downdraft ventilation tends to suppress convection in the upshear quadrants—the same part of the TC where balanced downward motions (i.e., another form of downdraft ventilation) act to suppress convection in a tilted vortex (Jones 1995; DeMaria 1996; Zawislak et al. 2016). Entrainment of this relatively low-θ_e air into eyewall updrafts downshear can result in shallower convection, less latent heating, a hydrostatic pressure rise in the eye, and reduced TC intensity (Riemer et al. 2013; Riemer and Laliberté 2015; Zhang and Rogers 2019).

In contrast to a lack of recovery, several studies provide evidence of enhanced surface fluxes counteracting the debilitating effects of downdraft ventilation, allowing for a complete recovery of low-θ_e air upon entry into eyewall updrafts (Tang and Emanuel 2012a; Tao and Zhang 2014; Juračić and Raymond 2016; Gao et al. 2017; Nguyen et al. 2019; X. Chen et al. 2021; Alland and Davis 2022). The likelihood of recovery increases for warmer SST environments (X. Chen et al. 2021), air that is closer to the sea surface (Wadler et al. 2021a), and more intense TCs (Finocchio and Rios-Berrios 2021). For early-stage storms that have not yet formed an eyewall, downdraft-cooled parcels that recover can ascend in the left-of-shear quadrants, develop into deep convection at the leading edge (i.e., cyclonically downwind) of a tilt-related convective precipitation shield, and contribute to eyewall formation (X. Chen et al. 2021).

2) RADIAL VENTILATION

Simpson and Riehl (1958) were the first, to the authors' knowledge, to document radial ventilation. Radial ventilation refers to the horizontal transport of low-θ_e air from the surrounding environment into the TC inner core by storm-relative radial inflow, horizontal eddy fluxes, or both (discussed further in the following two paragraphs). This can result in the reduced areal extent of convection in the inner core and acts as a constraint on the TC heat engine (Bender 1997; Shelton and Molinari 2009; Munsell et al. 2013; Shu et al. 2014; Nguyen et al. 2017; Alland et al. 2021a; Alland and Davis 2022).

Radial ventilation can occur in the mid- and upper troposphere via storm-relative inflow associated with the superposition of a tilted TC circulation in a vertically sheared background flow (Simpson and Riehl 1958; Willoughby et al. 1984; Marks et al. 1992; Bender 1997; Cram et al. 2007; Shelton and Molinari 2009; Davis and Ahijevych 2012; Nguyen et al. 2017; Alland et al. 2021b; Fischer et al. 2023; see Fig. 4b). Radial inflow maximizes upshear and right of shear (Corbosiero and Molinari 2003; Reasor et al. 2013; DeHart et al. 2014), which can transport low-θ_e air into the TC inner core. If the radial ventilation occurs in upper levels where the TC warm anomaly is generally most prominent, it has been hypothesized to result in a top-down weakening of the TC by inducing a hydrostatic increase in the surface pressure, a decrease in troposphere-mean diabatic heating, and a weakening of the mean secondary circulation (Gray 1968; Frank and Ritchie 2001; Kwon and Frank 2008; Fu et al. 2019).

Radial ventilation in midlevels can also be associated with shear-induced eddies that are excited in response to a TC's

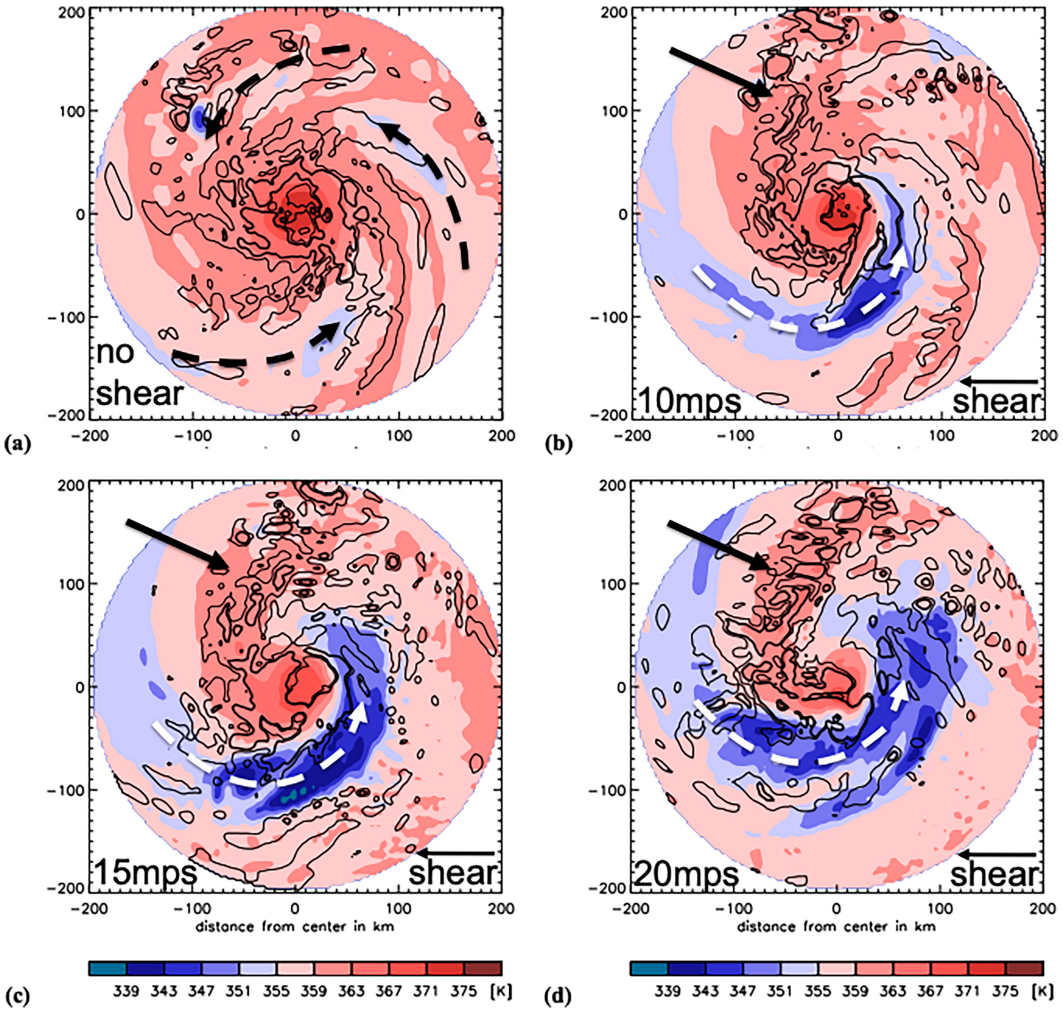

FIG. 3. Boundary layer θ_e (color; averaged over the lowest 1 km), and upward motion (thin contour: 0.2 m s^{-1}; thick contour: 1 m s^{-1}, averaged between 1.25 and 2 km height) at 5 h in the idealized simulations of Riemer et al. (2010). The center of the TC averaged over the lowest 2 km is in the middle of the domain. (a) The no_shear case, and the (b) 10, (c) 15, and (d) 20 m s^{-1} shear cases. The shear direction is indicated in the lower-right corner of each plot. Solid arrows highlight the quasi-stationary convective asymmetry outside of the eyewall in the shear cases and dashed white arrows show the quasi-stationary region of depressed boundary layer θ_e air. The dashed black arrows indicate transient bands of less-reduced θ_e values in the no_shear case. The depicted times are representative for the early part of the experiments [adapted from Fig. 7 in Riemer et al. (2010)].

vertical tilt (e.g., Cram et al. 2007; Tang and Emanuel 2010, 2012a). This ventilation pathway, which is shown conceptually in Fig. 5 along with the downdraft ventilation pathway described above, locally decreases θ_e within the upward branch of the secondary circulation. In axisymmetric models of TCs with parameterized radial ventilation, this type of radial ventilation is capable of weakening TCs in environments that, by all other measures, favor intensification (Tang and Emanuel 2010, 2012b).

The extent to which radial and downdraft ventilation disrupts a TC depends not only on the magnitude of VWS, but also on the environmental humidity. A TC is more likely to resist ventilation if the air being transported from the surrounding environment into the inner core has higher θ_e (Tang and Emanuel 2010; Alland et al. 2021a,b). Tang and Emanuel (2012b) created a ventilation index that combines environmental VWS, the entropy deficit of the surrounding midlevel environment, the air–sea vapor pressure deficit, and the potential intensity. This index is able to distinguish environments that are favorable for developing versus nondeveloping TCs. Larger and more intense TCs are also more resilient to radial ventilation because the stronger and more expansive tangential wind field increases the inertial stability of the vortex and thereby prevents radial intrusions of air parcels from the surrounding environment with relatively lower θ_e into the inner core (Riemer and Montgomery 2011; Finocchio and Rios-Berrios 2021).

Radial and downdraft ventilation can work together to affect TC structure and intensity. In the middle and upper troposphere, dry air from radial ventilation (Fischer et al.

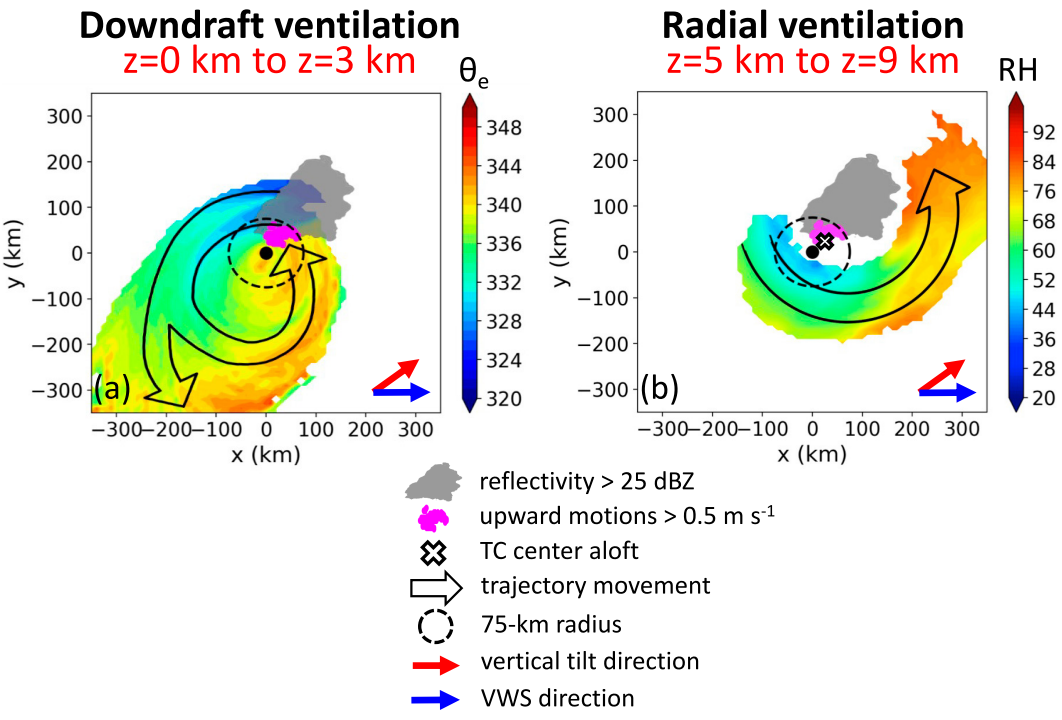

FIG. 4. Conceptual diagrams of ventilation pathways showing, in shading, the (a) average equivalent potential temperature (K) of trajectories initialized in downdraft ventilation regions between heights of 0 and 3 km and (b) average RH (%) of trajectories initialized in radial ventilation regions between heights of 5 and 9 km. Other information includes reflectivity greater than 25 dBZ (gray shading), upward motions greater than 0.5 m s^{-1} (magenta dots), the TC center averaged between heights of 5 and 9 km (white ×), parcel movement (black arrows), the inner 75 km (dashed circle), the vertical tilt direction from the surface to 6 km (red arrow), and the VWS direction (blue arrow). [Adapted from Fig. 17 of Alland et al. (2021a) and Fig. 13 of Alland et al. (2021b).]

2023), as well as convergence of storm-relative inflow with the TC's upper-tropospheric outflow upshear (Dai et al. 2021), can result in troposphere-deep subsidence (i.e., downdraft ventilation). These combined ventilation pathways dry and stabilize the upshear TC inner core. In the lower and middle troposphere, descending radial inflow from rainband activity can flush lower-θ_e air into the subcloud layer, reduce the areal extent of convection in the inner core, and limit TC development (Barnes et al. 1983; Powell 1990; Hence and Houze 2008; Didlake and Houze 2009, 2013) (see Fig. 4a).

3) Relative importance of ventilation pathways

The relative importance of the downdraft and radial ventilation pathways in modulating a TC's convective structure and intensity remains an open question, and may be case dependent. Alland et al. (2021a) showed in idealized simulations that downdraft and radial ventilation can operate at the same time, while Alland and Davis (2022) showed in simulations of Hurricane Michael (2018) that downdraft ventilation preceded radial ventilation in limiting TC development. Riemer et al. (2010) and Riemer and Laliberté (2015) suggested that downdraft ventilation at low levels may be more destructive to TC development than radial ventilation above the boundary layer because downdraft ventilation directly impacts the energy cycle of a TC in the subcloud layer where convection initiates. In addition, the inflowing air in the mid- and upper troposphere associated with radial ventilation may be deflected by the TC's swirling winds, effectively limiting its destructive potential (Willoughby et al. 1984; Riemer and Montgomery 2011). For weaker TCs, though, this deflection may be less prominent, resulting in stronger interaction between the environment and the inner core (Alland et al. 2021b; Finocchio and Rios-Berrios 2021). Tang and Emanuel (2012a) suggested that radial ventilation is less effective at interfering with the development of a TC when it occurs primarily in the upper levels because radial gradients of θ_e are smaller in the upper troposphere than in the lower and middle troposphere. However, Fu et al. (2019) showed that radial ventilation aloft can be particularly effective at weakening already intense TCs due to the combination of a well-developed warm core and stronger storm-relative flows in the upper levels compared to in the mid- and low levels.

The importance and timing of ventilation pathway(s), or a TC's resiliency to ventilation, are likely dependent on the storm conditions (e.g., the size and intensity), and environmental conditions (e.g., the vertical and radial locations of the dry air and VWS) (Finocchio and Rios-Berrios 2021). Despite our improved understanding of ventilation, more research is

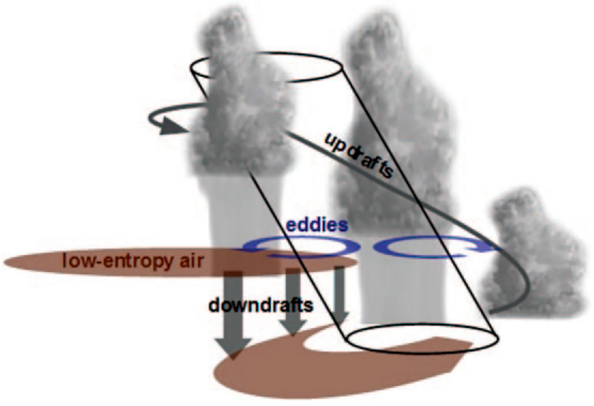

FIG. 5. A conceptual illustration of a TC undergoing two types of ventilation. Radial ventilation is depicted as horizontal eddies (blue arrows) that transport low-entropy air from the environment into eyewall convection of the tilted vortex. Downdraft ventilation is depicted by gray arrows labeled "downdrafts," which are the result of precipitation falling from the asymmetric convection in the tilted TC into subsaturated air below. Regions of low-entropy air in the midlevels and in the subcloud layer are denoted by brown shading [adapted from Fig. 1 in Tang and Emanuel (2012b)].

still needed to better understand why ventilation negatively affects some TCs and has only a limited effect on others.

d. *Boundary layer asymmetries*

Deep-layer VWS also introduces distinct thermodynamic and kinematic asymmetries within the TC boundary layer. As a consequence of the aforementioned effects of downdraft ventilation and subsequent boundary layer recovery, θ_e is generally lowest in the left-of-shear quadrant and highest in the downshear-right quadrant (e.g., Riemer et al. 2010; Zhang et al. 2013; Nguyen et al. 2017; X. Chen et al. 2019; Alland et al. 2021a). The downdraft-modified boundary layer parcels enhance surface enthalpy fluxes left of shear, enabling a subsequent boundary layer recovery of these low-θ_e parcels. Thus, a wavenumber-1 asymmetry in the azimuthal distribution of θ_e and surface enthalpy fluxes has been observed in sheared TCs (Zhang et al. 2013; Nguyen et al. 2019). These boundary layer asymmetries can rotate cyclonically during vortex precession, especially for weak TCs.

The amplitude of the wavenumber-1 asymmetry in boundary layer θ_e is related to factors other than just the magnitude of VWS (Riemer et al. 2010; Nguyen et al. 2019; Wadler et al. 2022). A composite analysis of dropsondes collected in relatively weak TCs showed that TCs with higher intensification rates have larger values of surface enthalpy fluxes in the upshear quadrants compared to the downshear quadrants (Nguyen et al. 2019). TCs in environments with a southerly component of VWS have also been found to have a larger wavenumber-1 asymmetry in boundary layer θ_e outside of the radius of maximum winds than TCs in environments with a northerly component of VWS (Wadler et al. 2022). This asymmetry likely results from the superposition of large-scale advection of θ_e on the shear-induced θ_e asymmetries.

For the kinematic boundary layer structure, both observational and modeling studies (Zhang et al. 2013; Gu et al. 2016; Zhang et al. 2023) indicate that the boundary layer height, either represented by inflow layer depth or the height of maximum tangential wind, tends to increase with radius in each shear-relative quadrant. The boundary layer inflow is strongest and deepest in the downshear quadrants (Fig. 6), which is aligned with the location of the downshear convergence zone. However, the strongest tangential winds are located to the left of shear (Zhang et al. 2013; Rogers et al. 2015; Gu et al. 2016). Thermodynamically, the boundary layer inflow is an ideal conduit to bring low-θ_e parcels into the inner-core convection [section 2c and Ahern et al. (2021)]. However, the inflow also can accelerate the tangential wind in the downshear-left quadrant through the inward advection of absolute angular momentum and immediately downwind through azimuthal advection, while the tangential winds in the right-of-shear quadrants steadily weaken. In fact, Gu et al. (2016) found that during the initial weakening stage of modeled TCs in VWS, the left-of-shear tangential winds can continue to intensify for a few hours while the tangential winds to the right of shear decay.

Given that the TC boundary layer is relatively undersampled with in situ observations, more research is needed to understand the shear-induced asymmetries within that layer. The evidence discussed herein suggests that VWS induces both thermal and kinematic boundary layer asymmetries. Those asymmetries can have important implications by, for example, determining the location of maximum near-surface winds. Their effects on turbulent aspects that affect mixing and updraft development should also be investigated.

3. Compound effects of VWS and other factors on TC structure and intensity

While many studies have isolated the effects of VWS *magnitude* on TC structure and intensity, that metric alone cannot fully capture the myriad ways in which a TC responds to a given environment. Additional external factors—including details of the environmental wind profile, the relative direction of surface flow with respect to the shear direction, environmental moisture, and underlying SSTs—also influence vortex and precipitation asymmetries that emerge under VWS. This section discusses interactions between VWS magnitude and those factors with the goal of exposing the complex nature of TC–VWS interactions.

a. *Details of the wind profile*

The magnitude of the deep-layer VWS is often the only metric used to characterize how favorable an environmental wind profile is for TC intensification. Historically, this was due to a paucity of real-time satellite-derived atmospheric motion vectors in the middle troposphere, which hindered operational estimates of shear in layers other than 200–850 hPa (Velden and Sears 2014). However, details of the environmental wind profile beyond the deep-layer shear magnitude can have a strong influence on TC structure and intensity.

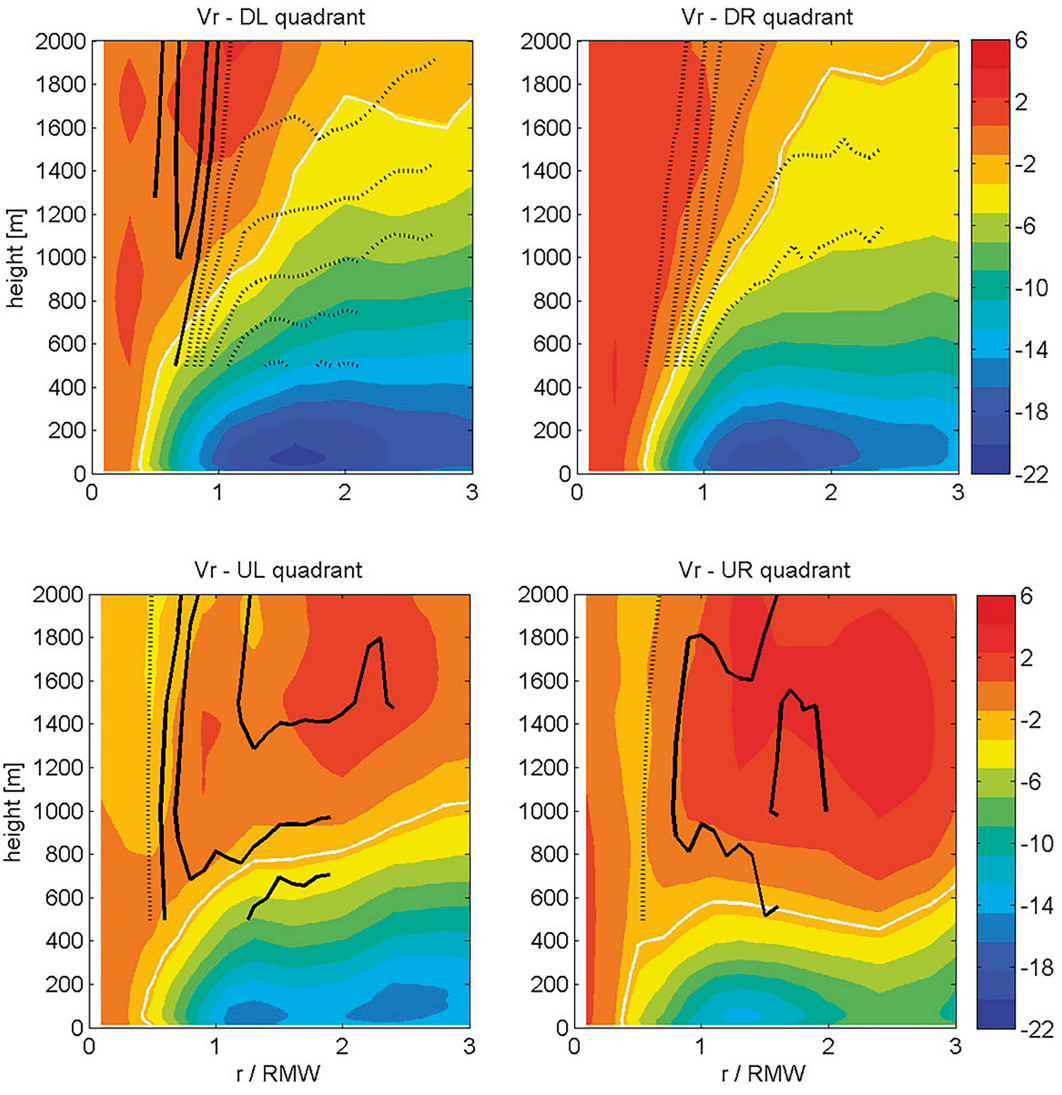

FIG. 6. Dropsonde composites of the relative radial wind velocity (shaded; every 2 m s^{-1}) as a function of altitude and the normalized radius to the storm center for the four quadrants relative to the shear direction. The white line in each panel represents the height of 10% peak inflow. Doppler radar composite results are shown in the black lines with solid lines representing outflow and dotted lines representing inflow with a contour interval of 0.5 m s^{-1} [adapted from Fig. 4 of Zhang et al. (2013)].

Studies primarily focused on TC genesis have explored whether the impacts of VWS on developing disturbances depend on the shear direction. Tuleya and Kurihara (1981) found that easterly shear was more favorable for genesis than westerly shear of the same magnitude, which they argued was due to easterly shear allowing for greater coupling between the upper and lower parts of westward-propagating disturbances within the deep tropics. The intrinsic northwesterly beta shear of the TC vortex partially offsets easterly environmental shear, which could also explain why easterly shear has been found to be less destructive to a TC than the same magnitude of westerly shear (Ritchie and Frank 2007). Statistical studies based on large samples of cyclogenesis and postgenesis TC cases are mostly consistent with the result that easterly shear is more favorable for genesis and intensification than westerly shear (Zeng et al. 2010; Nolan and McGauley 2012). However, in idealized simulations on the beta plane that isolate the impact of shear direction from factors such as maximum potential intensity, Nolan and McGauley (2012) found westerly shear was actually more favorable for genesis than easterly shear. This suggests that easterly shear only appears to be more favorable for TC genesis because it tends to occur in regions where other environmental factors such as SST are also favorable. The shear direction sensitivity may also differ for genesis cases compared to more developed TCs. Wei et al. (2018) found that, for postgenesis TCs in the western North Pacific, westerly shear was more strongly correlated with short-term weakening than easterly shear after controlling for SST.

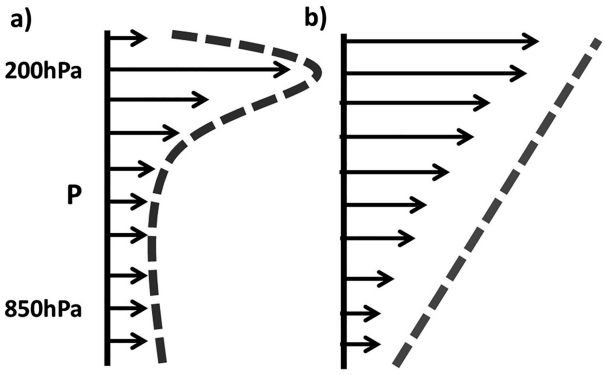

FIG. 7. Schematics of two vertical wind profiles typical of environmental flow regimes that impinge on TCs but provide identical 200–850 hPa wind shear values as traditionally calculated: (a) a wind profile commonly associated with low-latitude systems with the strongest upper-tropospheric winds concentrated in a shallow layer and (b) a linearly distributed wind profile over a deep layer as might exist poleward of the deep tropics and associated with transient midlatitude troughs [adapted from Fig. 1 in Velden and Sears (2014), and reproduced from Fig. 11 in Elsberry and Jeffries (1996)].

The vertical distribution of shear through the troposphere can also influence TC development. Elsberry and Jeffries (1996) described two hypothetical wind profiles with the same deep-layer shear: one with all of the shear concentrated in the upper troposphere (Fig. 7a), and the other with shear linearly distributed through the depth of the troposphere (Fig. 7b). They hypothesized that the upper-level shear profile is more favorable for TC development because the TC outflow can counteract upper-level shear, while more deeply distributed shear is more likely to tilt and ventilate the TC inner core. Ryglicki et al. (2018a) usefully pointed out that TC environments with deeply distributed shear (as in Fig. 7b) tend to be associated with upper-level troughs, while environments with upper-level shear (as in Fig. 7a) tend to be associated with upper-level anticyclones.

A consensus has yet to emerge on whether upper- or lower-level shear is more favorable for TC intensification. Finocchio et al. (2016) conducted idealized simulations exposing weak, symmetric vortices to environmental wind profiles with 10 m s^{-1} of westerly VWS maximized at different heights and extending through different depths of the troposphere. They found that shear concentrated lower in the troposphere was more destructive to a developing TC than upper-level shear because it tilted the vortices further downshear and caused stronger downward fluxes of low-θ_e air into the TC boundary layer from convective downdrafts. These findings are consistent with earlier (Frank and Ritchie 1999) and subsequent (Ryglicki et al. 2018b) modeling studies that involved experiments exposing developing TCs to different vertical distributions of VWS.

In contrast to these studies, Xu and Wang (2013) and Fu et al. (2019) exposed mature hurricanes to different wind profiles with 10 m s^{-1} of easterly VWS and found that simulated TCs in upper-level shear weakened more and exhibited stronger inner-core asymmetries than the TCs in lower-level shear. Fu et al. (2019) attributed the greater weakening in upper-level shear to stronger upper-level ventilation of the warm core. They hypothesized that upper-level shear is less destructive to the weak TCs examined in previous modeling studies because the weaker storms are too shallow to be exposed to the strongest storm-relative flows aloft (e.g., Nam and Bell 2021). However, more research is needed to understand the different responses to upper- versus lower-level shear and how they might relate to shear direction and aspects of the TC vortex.

Statistical analyses of real sheared TCs have generally found that low-level shear is more commonly associated with weakening than upper-level shear (Zeng et al. 2010; Wang et al. 2015). However, Finocchio and Majumdar (2017b) did not find a clear relationship between TC intensity change and their metrics describing the vertical distribution of VWS. These contradictory findings could be due to differences in the metrics used to define the VWS height and/or the geographic focus areas among the different statistical studies. The vertical distribution of VWS may also have a larger and more consistent impact on the intensity of developing disturbances and weak TCs compared to the more developed storms considered in these studies. More detailed statistical and observational analysis of weak and developing storms is needed to better understand the apparent disagreements regarding the impacts of different VWS profiles on TC intensity change.

Different multidirectional shear flows can also have distinct impacts on TC intensity and structure. In the midlatitudes, environments with winds that rotate clockwise with altitude (positive helicity) favor stronger and longer-lived convective updrafts (Davies-Jones et al. 1990). Positive TC-relative environmental helicity is also more favorable for TC intensification. Nolan (2011) and Onderlinde and Nolan (2014) used idealized simulations of TCs in horizontally uniform environments with a mean wind vector that rotates either clockwise (positive helicity) or counterclockwise (negative helicity) with increasing altitude. Both studies found the clockwise-rotating wind profile (positive helicity) resulted in more TC intensification, despite all experiments having the same deep-layer VWS magnitude.

Onderlinde and Nolan (2016) reasoned that positive helicity is more favorable for TCs than negative helicity because, in their simulations, air parcels ingested into downshear convective updrafts experienced more warming and moistening via surface enthalpy fluxes in positive helicity environments. However, Gu et al. (2018) demonstrated that balanced (dry) dynamics alone can explain why positive helicity is more favorable for TC development: a clockwise-rotating environmental wind profile advects the lower part of the vortex azimuthally downwind of the overall vortex tilt vector, resulting in a superposition of positive local helicity and balanced ascent associated with the tilted vortex. This configuration promotes the propagation of convection toward the upshear quadrants. In identical experiments but with active moist physics, diabatic heating in convection keeps the moist vortices more vertically coupled than in the corresponding dry simulations (Gu et al. 2019). Moreover, the favorable configuration of vortex tilt and convection established early in the

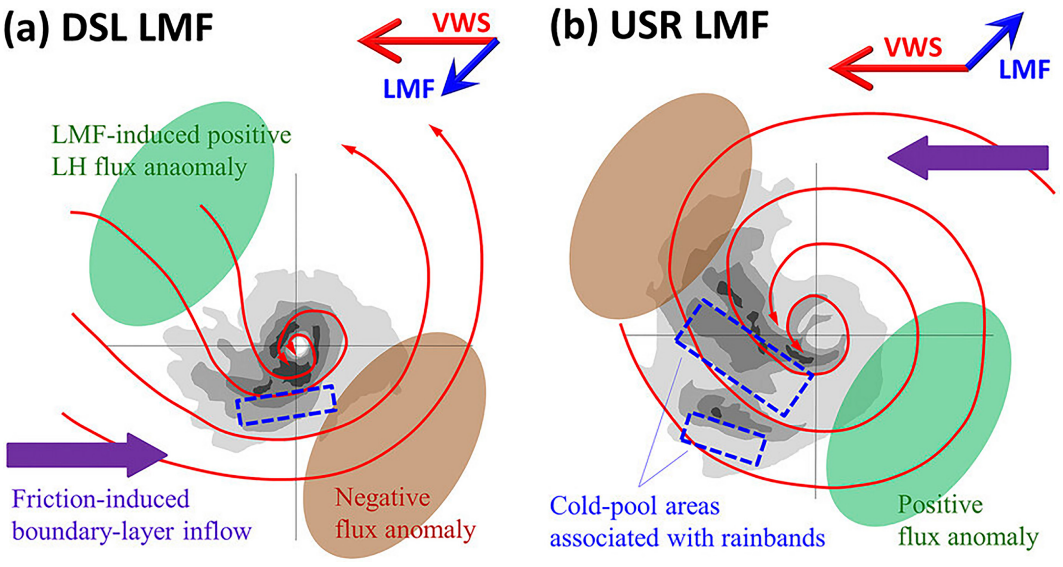

FIG. 8. Conceptual models showing the responses of a Northern Hemisphere TC to (a) downshear-left (DSL) low-level mean flow (LMF) and (b) upshear-right (USR) LMF. Gray shading indicates radar reflectivity. Red streamlines represent the boundary layer trajectories in a shear-relative coordinate system [adapted from Fig. 1 of B.-F. Chen et al. (2021)].

experiments sets up a positive feedback with diabatic heating in convection that allows for the faster upshear precession of vortices in positive-helicity environments. In other words, favorable dry dynamics set the stage for subsequent convective feedbacks that hasten vortex alignment in multidirectional shear environments with positive helicity. Collectively, these model-based results suggest that, with all else being equal, TCs in negative helicity environments are more likely to remain misaligned than TCs in unidirectional shear or positive helicity environments.

b. *Surface flow*

The surface flow in the TC environment modulates the TC intensity and structural response to VWS by influencing the horizontal distribution of boundary layer convergence and surface enthalpy fluxes. The distribution of low-level convergence around a TC partly determines where the stationary rainband complex forms (Willoughby et al. 1984; Riemer 2016), while the surface enthalpy fluxes determine the extent of thermodynamic recovery of downdraft air parcels in the TC boundary layer (Powell 1990). Riemer and Montgomery (2011) also demonstrated how storm-relative surface flow distorts the circulation in the lower levels of a TC, determining the extent to which environmental air is able to reach the inner core.

Only recently have the combined effects of low-level flow and VWS on TC structure and intensity been explored systematically. Rappin and Nolan (2012) showed that surface flow counteraligned with the shear vector is more favorable for TC genesis than surface flow aligned with the shear vector. In the counteraligned scenario, the superposition of the vortex circulation and the surface wind results in a surface wind maximum to the left of the shear vector, which increases surface enthalpy fluxes ahead of the asymmetric convective complex. This favors the upshear propagation of asymmetric convection, leading to a more rapid reduction in vortex tilt.

B.-F. Chen et al. (2018) examined a wide array of low-level flow orientations relative to the deep-layer shear vector using analysis and observational composites of postgenesis TC cases. They found low-level flow directed toward the right of shear favors expansion of the 34-kt (17.5 m s^{-1}) wind radius, while low-level flow directed toward the left of shear favors intensification. They conducted idealized simulations to explore the reasons for this result and found that low-level flow pointing toward the upshear-right quadrant favors wind-field expansion because of enhanced rainband activity (B.-F. Chen et al. 2019; Fig. 8b). The opposite orientation of the low-level flow relative to the shear vector increases the mean low-level inflow downshear and the humidity of air parcels ingested into inner-core convection. This promotes intensification through the earlier development of a symmetric eyewall (Fig. 8a). Similar to Rappin and Nolan (2012), upshear-oriented low-level flow generally favored intensification more than downshear low-level flow in the B.-F. Chen et al. (2019) study, but only in their simulations over a warmer prescribed SST. However, comparisons between these two studies is complicated by the fact that Rappin and Nolan (2012) conducted their simulations in radiative–convective equilibrium environments, where warmer SST results in higher saturation deficits that must be overcome in order for genesis to occur. In a follow-up analysis of real TC cases, B.-F. Chen et al. (2021) showed that TC intensification is favored in environments with low-level flow directed toward the downshear-left quadrant regardless of the background SST, deep-layer shear magnitude, or environmental humidity.

Lee et al. (2021) conducted similar simulations to B.-F. Chen et al. (2019), except they imposed the shear and the different low-level flows on more mature TCs. They found that for these more intense storms, the low-level flow associated with the fastest intensification is directed upshear left (cf. downshear left in B.-F. Chen et al. 2019). This low-level flow orientation results in surface fluxes maximized downshear, which invigorates upshear-left convection and promotes a more symmetric diabatic heating structure.

c. *Environmental moisture*

The tropics generally have a minimum in θ_e near 700 hPa (Jordan 1958; Ooyama 1969; Dunion 2011). As such, moistening of the lower and middle troposphere is necessary for the development and sustenance of deep convection within the TC vortex (Gray 1968; Emanuel 1989; Bister and Emanuel 1997; Nolan 2007; Raymond et al. 1998; Rappin et al. 2010; Komaromi 2013; Zawislak and Zipser 2014; Helms and Hart 2015; Rios-Berrios et al. 2016b). In idealized simulations of weak TCs in environments with no VWS, Braun et al. (2012) showed that a layer of dry air between 850 and 600 hPa could only limit TC intensification when it was initialized very close to the storm center. Dry air can only weaken a TC if it is able to penetrate into the inner core to reduce the upward vertical mass flux and convergence of angular momentum in the subcloud layer (Montgomery and Smith 2014; Tang and Zhang 2016; Alland et al. 2017). If dry air does not penetrate into the inner core, it can still reduce convection outside the moist region (Tao and Zhang 2014), which can reduce the radial extent of the moist envelope and leave a TC more vulnerable to subsequent dry air intrusions (Kimball 2006; Hill and Lackmann 2009; Braun et al. 2012).

The combination of VWS and dry air around a vortex can be particularly effective at limiting TC intensification of weak TCs (Tang and Emanuel 2012a; Molinari et al. 2013; Tao and Zhang 2014; Rios-Berrios et al. 2016a,b; Rios-Berrios and Torn 2017; Nguyen et al. 2017, 2019; Alland et al. 2021a). For example, Molinari et al. (2013) analyzed observations of a tropical storm under strong VWS (11–15 m s^{-1}) and exceptionally dry air (15% relative humidity). The tropical storm remained fairly asymmetric and weak, which Molinari et al. (2013) hypothesized was a result of radial and downdraft ventilation through the combination of strong VWS and dry environmental air. Nguyen et al. (2017) also attributed the asymmetric convective structure of Tropical Storm Cristobal (2014) to the combination of dry air and strong VWS. In general, as environmental relative humidity decreases, the likelihood for radial and downdraft ventilation increases (Riemer et al. 2010, 2013; Alland et al. 2021a,b).

The location of dry air with respect to the VWS is also important. Ge et al. (2013) found in idealized simulations that midtropospheric dry air initially located to the right of the shear vector is advected by the TC's cyclonic flow toward the downshear quadrants, where it limits convection and thwarts the realignment of a tilted TC vortex. Consistent with this result, Rios-Berrios et al. (2016b) found in an ensemble simulation of a moderately sheared TC that members simulating a stronger storm had higher humidity in the lower troposphere to the right of shear. In composites of moderately sheared TCs, Rios-Berrios and Torn (2017) found that intensifying storms have higher midtropospheric relative humidity upshear compared to steady-state or weakening storms. Rios-Berrios and Torn (2017) suggest that the higher humidity upshear may reduce midlevel dry air intrusions and allow for a more axisymmetric distribution of convection. Source regions of dry air entering the TC inner core at a particular level are closely related to the environmental storm-relative flow. For example, the flow topology of a TC in westerly storm-relative flow favors environmental intrusions from the northwest quadrant (Riemer and Montgomery 2011). The inner cores of stronger TCs are also more insulated from intrusions of environmental air than weak TCs. However, more research is needed to better understand the dependence of TC structure and intensity change on different configurations of VWS and dry air, including the altitude and azimuthal location of dry air relative to the strongest storm-relative flows (i.e., ventilation).

d. *Sea surface temperature*

The underlying ocean temperatures, commonly characterized by the sea surface temperature (SST), also affect the outcome of TC–VWS interactions. Studies have identified two contrasting SST impacts on sheared TCs: a positive impact of higher SST on TC development through enhanced surface fluxes (Tao and Zhang 2014; X. Chen et al. 2018a, 2021; Alland and Davis 2022; Schecter 2022), and a perhaps less-intuitive negative impact of higher SST mainly found under radiative–convective equilibrium (RCE) conditions (Nolan and Rappin 2008; Rappin and Nolan 2012).

With higher SST, the low-θ_e air flushed into the boundary layer via shear-induced downdrafts [section 2c(1)] is refueled by surface fluxes more rapidly before becoming entrained in inner-core convection. The enhanced surface fluxes thereby reduce the effect of downdraft ventilation and strengthen the connection between the midlevel and low-level vortices (Tao and Zhang 2014; X. Chen et al. 2018a, 2021; Alland and Davis 2022). Meanwhile, higher SST excites more vigorous convective activity at larger radii, which broadens the vortex circulation and increases TC resistance to shear (Schecter 2022). The rate of tilt reduction is sensitive to SST such that the higher the SST, the faster reduction of tilt magnitude (Schecter 2022; Fig. 9).

In contrast, Nolan and Rappin (2008) found in idealized simulations of sheared TCs in RCE environments that higher SST can actually make a TC less resilient to VWS. They found that the higher SST increases the height of the freezing level, which in turn increases the altitude of the developing midlevel vortex. For the wind profile used in their simulations, the higher altitude of the midlevel vortex meant it was exposed to stronger storm-relative flow and shear-induced ventilation. In addition, Rappin et al. (2010) found that increasing SST in RCE simulations results in a drier midlevel environment and, hence, stronger ventilation due to shear at the altitude of the midlevel vortex. Although RCE may be a valid approximation for the large-scale tropical environment on

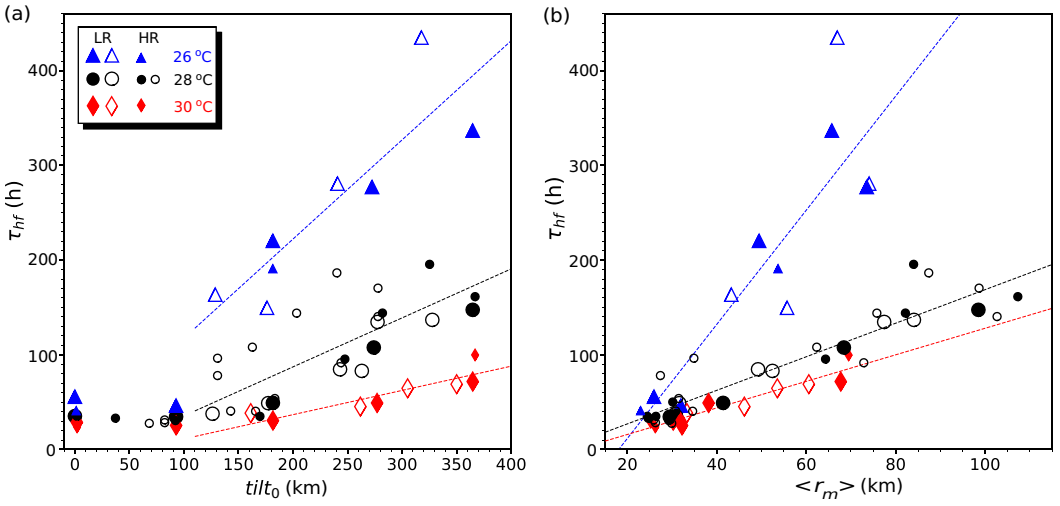

FIG. 9. (a) Length of the hurricane formation period (τ_{hf}) vs the initial tilt magnitude ($tilt_0$) from the idealized simulations of Schecter (2022). The color and shape of each symbol corresponds to the SST (legend). The dashed lines are linear regressions among all points in each SST group with $tilt_0 > 100$ km. (b) Relationship between τ_{hf} and the radius of maximum surface wind speed $\langle r_m \rangle$ time averaged during the hurricane formation period. Dashed lines are linear regressions as in (a), but over all data points within the pertinent SST group [adapted from Fig. 1 in Schecter (2022)].

daily time scales and longer, the local environment around TCs can be far from RCE. Therefore, more research is needed on the validity of the RCE assumption as it relates to TC–VWS interactions.

4. Pathways to TC development and intensification in shear

Despite the substantial body of research highlighting the predominantly negative impacts of VWS on TC structure and intensity discussed so far, VWS is not always destructive to a TC. An emerging line of research has sought to better understand the intensification of TCs in environments with VWS magnitudes that are neither too weak nor too strong (e.g., Molinari et al. 2004, 2006; Molinari and Vollaro 2010; Montgomery et al. 2010; Foerster et al. 2014; Stevenson et al. 2014; Rios-Berrios et al. 2016a,b; Zawislak et al. 2016; Nguyen et al. 2017; Ryglicki et al. 2018a; X. Chen et al. 2018a; Rogers et al. 2020; and many others). This range of VWS magnitudes is commonly referred to as "moderate shear." Four pathways to TC intensification under moderate shear have emerged from the literature: vortex tilt reduction, vortex reformation, axisymmetrization of precipitation, and outflow blocking. This section reviews each pathway separately even though they may not be mutually exclusive; for example, vortex tilt reduction may occur together with vortex reformation. These pathways most likely explain the intensification of weak, disorganized TCs (e.g., tropical depressions and tropical storms) into major hurricanes.

a. *Vortex tilt reduction*

Multiple studies have suggested that a nearly aligned vortex is often a precursor to TC intensification, including the onset of rapid intensification (Frank and Ritchie 2001; Reasor et al. 2004; Reasor and Eastin 2012; Rappin and Nolan 2012; Zhang and Tao 2013; Tao and Zhang 2014; Rogers et al. 2015; Nguyen and Molinari 2015; Rios-Berrios et al. 2016b, 2018; X. Chen et al. 2019; Rogers et al. 2020; Rios-Berrios 2020; Alvey et al. 2020; Schecter and Menelaou 2020; Nam et al. 2023). While the literature often uses the terminology "vortex realignment" to describe how a TC vortex evolves from being tilted to being nearly aligned, recent work (discussed below) has uncovered different pathways that explain such evolution. Therefore, we adopt the concept of "tilt reduction" herein to acknowledge the multiple processes that explain the transition from a tilted to a nearly aligned TC vortex.

Idealized TC simulations have been extensively used to study the relationship between VWS, vortex tilt, and TC intensity (Jones 1995; DeMaria 1996; Frank and Ritchie 1999, 2001; Jones 2000a,b, 2004; Patra 2004; Wong and Chan 2004; Kwon and Frank 2005, 2008; Rappin and Nolan 2012; Riemer et al. 2013; Zhang and Tao 2013; Tao and Zhang 2014; Miyamoto and Nolan 2018; Rios-Berrios et al. 2018; Tao and Zhang 2019; Rios-Berrios 2020; Schecter and Menelaou 2020; Schecter 2022; Nam et al. 2023). These simulations use models of varying complexities ranging from dry, nonhydrostatic models (Jones 1995; DeMaria 1996; Jones 2000a,b; Patra 2004; Wong and Chan 2004; Kwon and Frank 2005) to models that include moist processes (Flatau et al. 1994; Wang and Holland 1996; Frank and Ritchie 1999; Wong and Chan 2004; Kwon and Frank 2008; Rappin and Nolan 2012; Riemer et al. 2013; Zhang and Tao 2013; Tao and Zhang 2014; Miyamoto and Nolan 2018; Rios-Berrios et al. 2018; Tao and Zhang 2019; Rios-Berrios 2020; Ryglicki et al. 2018b; Schecter and Menelaou 2020; Schecter 2022; Nam et al. 2023). A cloud-free, vertically aligned TC-like vortex is usually specified in the initial conditions along with environmental flow and a thermodynamic sounding characteristic of the tropical atmosphere.

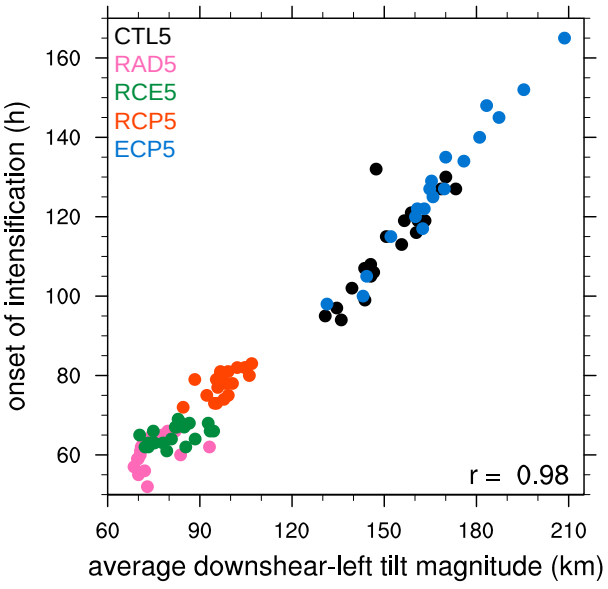

FIG. 10. Comparison between the onset of intensification and 400–900-hPa tilt magnitude averaged only during the time period when the tilt vector pointed downshear left (defined as a mathematical angle between 0° and 90°). Colors represent different 20-member ensembles with the same 5 m s^{-1} shear magnitude: a control configuration without radiation (CTL5; black), a configuration with radiation (RAD5; pink), a configuration in radiative–convective equilibrium (RCE5; green), a configuration with reduced cold pools (RCP5; orange), and a configuration with enhanced cold pools (ECP5; blue). The Pearson's correlation coefficient appears at the lower-right corner [adapted from Fig. 16 of Rios-Berrios (2020)].

The vortex is initially tilted toward the downshear quadrant, followed by an azimuthal rotation of the tilt vector toward the downshear-left and upshear-left quadrant. If the vortex is not completely sheared apart, intensification typically follows after a substantial reduction in tilt magnitude that typically coincides with a left-of-shear tilt configuration. For example, Fig. 10 shows that the onset of intensification in multiple idealized TC simulations is strongly correlated with the vortex tilt magnitude. This figure implies that for larger vortex tilt, the onset of intensification occurs later or becomes less likely.

Limited observational evidence also indicates that a small vortex tilt or tilt reduction precede intensification under moderate and strong VWS. Reasor and Eastin (2012) used the concept of "resiliency" to shear to describe TCs that maintain a small vortex tilt under moderate and strong VWS. Their observational analysis of Hurricane Guillermo (1997) showed that the persistent small vortex tilt explained (at least partly) how Guillermo was able to resist and intensify in strong VWS. Additional observational studies of individual TCs have also found a relatively small vortex tilt coinciding with intensification under moderate and strong VWS (e.g., Molinari et al. 2006; Stevenson et al. 2014; Rogers et al. 2015, 2020; Alvey et al. 2022). More recently, an observational analysis of hundreds of airborne Doppler radar analyses demonstrated that early-stage TCs with small vortex tilt were associated with greater rates of intensification (Fischer et al. 2024). Given that a tilted vortex is strongly coupled to convection (section 2a), satellite imagery has also provided evidence that a small vortex tilt precedes TC intensification (Ryglicki et al. 2018a, 2021).

The importance of vortex tilt reduction for TC intensification has motivated many studies aimed at identifying the physical processes responsible for changes in vortex tilt. As discussed in section 2a, early investigations focused on the role of dry dynamics. These studies found a preferred tilt orientation along—and to the left of—the VWS vector (Jones 1995; Wang and Holland 1996; Frank and Ritchie 2001; Reasor et al. 2004). Simulations with sheared barotropic vortices demonstrated that once the vortex tilts upshear, differential vorticity advection of the sheared flow acts to realign the vortex (Jones 1995). A different paradigm describes vortex tilt reduction through inviscid damping of vortex Rossby waves, which are excited by VWS (Reasor and Montgomery 2001; Schecter et al. 2002; Schecter and Montgomery 2003; Reasor et al. 2004; Reasor and Montgomery 2015). In this paradigm, the tilt evolution is described by a vortex Rossby wave asymmetry, often referred to as the "quasi mode" on a background azimuthally averaged flow. Moving outward from the TC center, a critical radius exists where the rotation rate of the background flow is equal to the precession frequency of the vortex tilt mode, where resonance between the two can occur. Stirring of the flow at this critical radius requires a damping of the vortex tilt at a rate proportional to the local vorticity gradient, provided the radial vorticity gradient is negative. While this mechanism invokes dry dynamics, additional studies (Schecter and Montgomery 2007; Reasor and Montgomery 2015) demonstrated that the location of the critical radius is dependent upon the static stability, or "cloudiness," of the TC core, with the critical radius shifting to smaller radii as static stability decreases. Thus, diabatic processes have been hypothesized to indirectly affect the vortex resilience by modifying the static stability and the TC's radial vorticity profile (Reasor et al. 2004).

More recent studies have emphasized the direct role of moist diabatic processes in vortex tilt reduction. Including moist processes in idealized simulations yields smaller vortex tilt magnitudes for otherwise similar but dry configurations, which led to the hypothesis that diabatic heating is important for vortex tilt reduction under VWS (Flatau et al. 1994; Wang and Holland 1996; Frank and Ritchie 1999). This hypothesis was challenged by Jones (2004), who demonstrated that TCs could experience a small vortex tilt in the absence of moist processes and that vortex tilt depends on the Rossby penetration depth and vortex strength. Yet, more recent studies that have relied on full-physics idealized TC simulations continue to emphasize the complex role of moisture and diabatic processes during vortex tilt reduction, especially in TCs below hurricane intensity. The main precipitating regions in these TCs is strongly coupled to the midtropospheric vortex, and their coevolution can reduce or amplify the vortex tilt induced by VWS (Rios-Berrios et al. 2018; Ryglicki et al. 2018b; B.-F. Chen et al. 2021). A substantial vortex tilt reduction happens through a relatively rapid restructuring of the TC vortex

(Miyamoto and Nolan 2018; Rios-Berrios et al. 2018; Rogers et al. 2020; Schecter and Menelaou 2020; Schecter 2022; Alvey and Hazelton 2022; Alvey et al. 2022), instead of through the gradual alignment of distinct lower and midlevel vorticity anomalies. This process may take several iterations (Ryglicki et al. 2018b), especially in marginal environments of moderate VWS and dry air (Nam et al. 2023).

During the restructuring process, convectively coupled vorticity anomalies aid the establishment of a nearly aligned and deep TC vortex (Miyamoto and Nolan 2018; Rios-Berrios et al. 2018). At the same time, precipitation transitions from being highly asymmetric to being more axisymmetric with an established eyewall. The established eyewall aids TC intensification through increased axisymmetric diabatic heating (Tao and Zhang 2014) while the nearly aligned vortex is more likely to intensify via surface heat fluxes (Molinari et al. 2004) and boundary layer vortex stretching (Rios-Berrios et al. 2018). Divergent outflow from the shear-induced convection also counteracts the sheared environmental flow (Ryglicki et al. 2018b, 2019, 2021). Observations and model simulations of real-world TCs support this restructuring process (Molinari et al. 2004; Rogers et al. 2020; Ryglicki et al. 2021; Alvey and Hazelton 2022; Stone et al. 2023), although the precise pathway to vortex tilt reduction can include vortex precession and vortex reformation in some cases (Alvey and Hazelton 2022). Vortex reformation is described in greater detail in the next subsection.

While vortex tilt reduction increases the likelihood that a TC will intensify, there is no consensus about the relationship between vortex tilt and intensity changes. In an observational composite analysis of TCs of hurricane intensity, Rogers et al. (2013) found no significant difference in the magnitude of vortex tilt between the intensifying and steady-state hurricanes. Some studies have also proposed that the onset of rapid intensification precedes a complete vortex alignment (e.g., Chen and Gopalakrishnan 2015; Judt et al. 2016; X. Chen et al. 2018a; Alvey et al. 2022). However, Fischer et al. (2024) found that vortex tilt is more important for intensity changes of TCs below hurricane intensity than for stronger TCs. These discrepancies could stem from differences in datasets (i.e., model simulations versus observations), challenges of defining and identifying vortex tilt, and the rapid evolution of convective processes, among other factors. Future work should seek to elucidate how external influences affect the relationship between TC intensity change and vortex tilt magnitude, and further explore cases that intensify prior to substantial tilt reduction.

b. *Reformation*

Observational and modeling studies have indicated that early-stage TCs (including tropical depressions, tropical storms, and category-1 hurricanes) are able to resist moderate to strong VWS by generating a new vorticity core or low-level circulation beneath or near the midlevel circulation in the downshear quadrant. This pathway has been termed downshear reformation (Molinari et al. 2004, 2006), and occurs most frequently for tropical storms (e.g., Davis et al. 2008; Molinari and Vollaro 2010; Nguyen and Molinari 2012; X. Chen et al. 2018a; Rogers et al. 2020; Alvey and Hazelton 2022). In this pathway, a broad and relatively weak parent TC circulation and the resulting weak axisymmetrization allow the development of a reformed vorticity core in a region of sustained diabatic heating (Schecter 2020). Downshear reformation notably alters the vortex structure and the thermodynamic state within the core, as a more compact and vertically aligned TC inner core forms in a more humid downshear environment. This sets up a more favorable configuration for TC intensification and, sometimes, rapid intensification. How fast a TC will intensify has been found to depend on the vortex tilt and the saturation fraction within the core after reformation (X. Chen et al. 2019). As reformation and the related structural changes occur within a few hours, they remain extremely difficult to observe and predict. The reformation can also change the steering flow the TC feels due to the center relocation, which has a long-term impact on the track forecasts. Thus, it is not surprising to see large forecast errors for both track and intensity when downshear reformation occurs (e.g., X. Chen et al. 2018a; Alvey et al. 2022; Rivera-Torres et al. 2023).

The development of the reformed vorticity core relies crucially on the stretching, tilting, and upward advection of vorticity through convective processes (Nguyen and Molinari 2015; X. Chen et al. 2018a; Rogers et al. 2020). The timing of reformation is thereby intrinsically dependent on the factors affecting the downshear convective activity, including TC intensity, VWS magnitude, and thermodynamic instability. The preference for reformation to occur at tropical storm intensity suggests that the new vortex can become the dominant vortex when the preexisting circulation is relatively weak. The presence of moderate to strong VWS also implies that sufficiently strong balanced lifting (cf. Jones 1995) and Ekman-like pumping (Schecter 2022) in the downshear region are important prerequisites, especially in the scenario where the surface enthalpy flux is nearly zero (Davis et al. 2008).

Another favorable condition for reformation is the counter-aligned surface wind and deep-layer VWS, which positions the maximum surface wind left of shear such that the enhanced surface enthalpy fluxes can support stronger asymmetric convection (X. Chen et al. 2018a). The timing of reformation is also related to a downshear environment characterized by weak instability (Raymond et al. 2011) and high column moisture (Rivera-Torres et al. 2023). Such conditions favor bottom-heavy mass flux profiles and low-level vorticity stretching (Rios-Berrios et al. 2018; Rogers et al. 2020; Stone et al. 2023), which can be an outcome of several previous episodes of deep convection. These episodes of deep convection can induce the formation of multiple mesovortices that propagate downstream (X. Chen et al. 2018a); however, only the mesovortex that successfully grows in size and strength with time becomes the reformed inner vortex (e.g., mesovortex C in Fig. 11) whereas the other mesovortices weaken after leaving the downshear convergence zone (Wang et al. 2022). In some cases, convective processes leading to reformation can benefit from diurnal, radiative influences (Alvey and Hazelton 2022), or interactions with island topography (Alvey et al. 2022). Despite these insightful findings, more research utilizing different observational platforms and high-

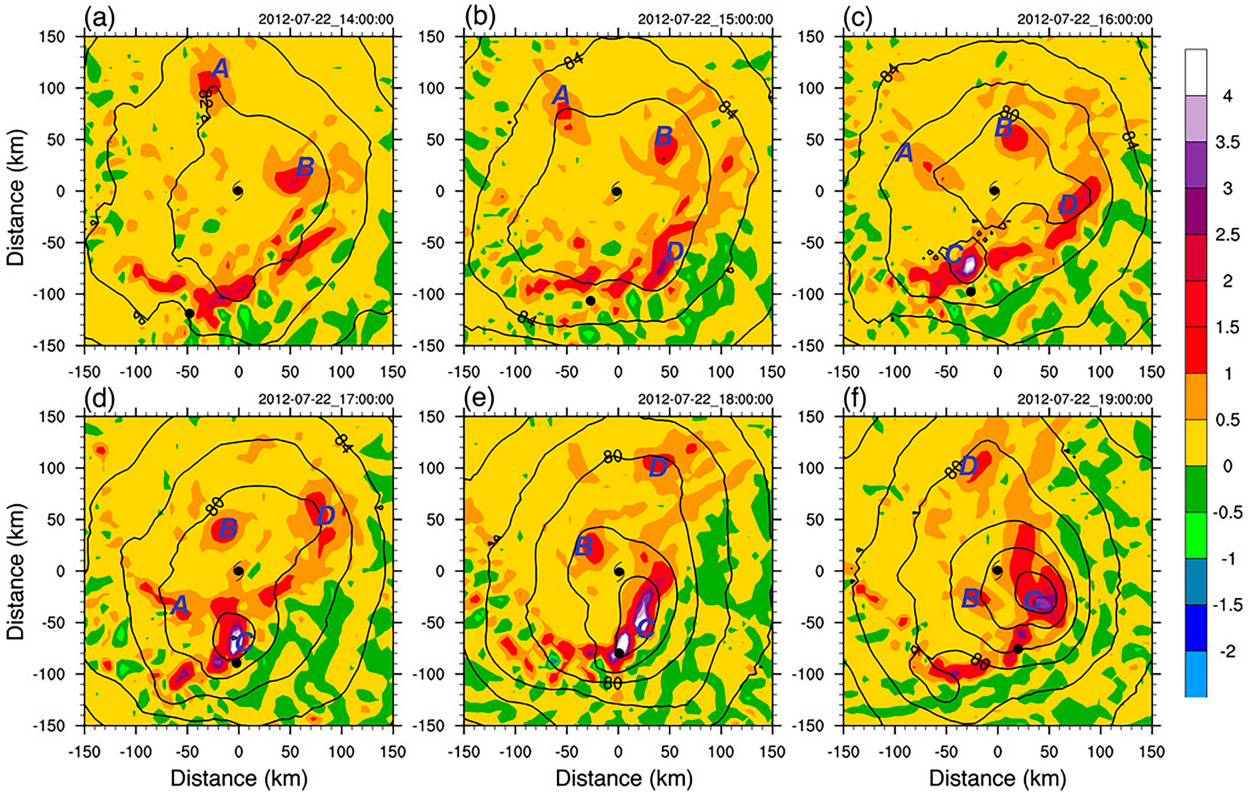

FIG. 11. Hourly evolution of 900 hPa relative vorticity (shading; 10^{-3} s^{-1}) and geopotential height (contoured every 2×10^2 gpm) from (a) 1400 to (f) 1900 UTC 22 Jul. The black hurricane symbol (dot) in each panel denotes the surface (500 hPa) TC center. Labels A–D denote different mesovortices, and mesovortex C becomes the reformed inner vortex of simulated Typhoon Vicente (2012). The 200–850 hPa VWS is heading southwest. [from Fig. 7 in Chen et al. (2018a)].

resolution numerical simulations is needed to quantify the frequency and predictability of vortex reformation.

c. *Precipitation axisymmetrization*

From a kinematic perspective, TC intensification requires the inward advection of angular momentum surfaces across the location of the radius of maximum wind within the boundary layer (e.g., Smith et al. 2009; Montgomery and Smith 2014; Smith and Montgomery 2015). This process is typically achieved due to sufficient diabatic heating within the TC inner core; however, as previously discussed, the pattern of diabatic heating in sheared TCs is asymmetric. Some studies have hypothesized TC intensification can be achieved through asymmetric processes, such as the injection of high-entropy air from the low-level TC eye into the eyewall region (e.g., Persing and Montgomery 2003; Cram et al. 2007; Reasor et al. 2009), the mixing of momentum between the TC eye and eyewall (Schubert et al. 1999; Kossin and Schubert 2001; Rozoff et al. 2009), or sufficiently intense asymmetric convection with robust warming via compensating subsidence (e.g., Heymsfield et al. 2001; Guimond et al. 2010; Nguyen and Molinari 2012; Guimond et al. 2016; Rogers et al. 2016; Hazelton et al. 2017; Wadler et al. 2018). Intense asymmetric regions of convection can also spin up the TC primary circulation via the axisymmetrization of local potential vorticity anomalies (e.g., Möller and Montgomery 2000; Hendricks et al. 2004; Montgomery and Smith 2014).

Nevertheless, through the use of dry, idealized simulations of hurricane-like vortices, Nolan et al. (2007) demonstrated TC intensification is significantly more responsive to the axisymmetric projection of heating than localized, asymmetric heating. Consistent with this idea, an increasing number of studies have begun to identify a relationship between the TC intensification rate and the degree of precipitation axisymmetry. For instance, multiple observational case studies of TCs in shear have linked TC intensification to increases in upshear precipitation and more axisymmetric convective structures (e.g., Stevenson et al. 2014; Rogers et al. 2015; Susca-Lopata et al. 2015; Zawislak et al. 2016; Rogers et al. 2016; Munsell et al. 2021). Additional studies of multiple TC cases have corroborated these results, showing that TCs with more axisymmetric precipitation structures tend to intensify more rapidly (e.g., Harnos and Nesbitt 2011; Jiang and Ramirez 2013; Zagrodnik and Jiang 2014; Alvey et al. 2015; Tao and Jiang 2015; Harnos and Nesbitt 2016; Tao et al. 2017; Fischer et al. 2018; Ryglicki et al. 2018a). Using a satellite-based precipitation partitioning scheme, Tao et al. (2017) indicated an increase in stratiform precipitation—especially in the upshear quadrants—was particularly important for the initiation of rapid intensification. Tao et al. (2017) hypothesized the

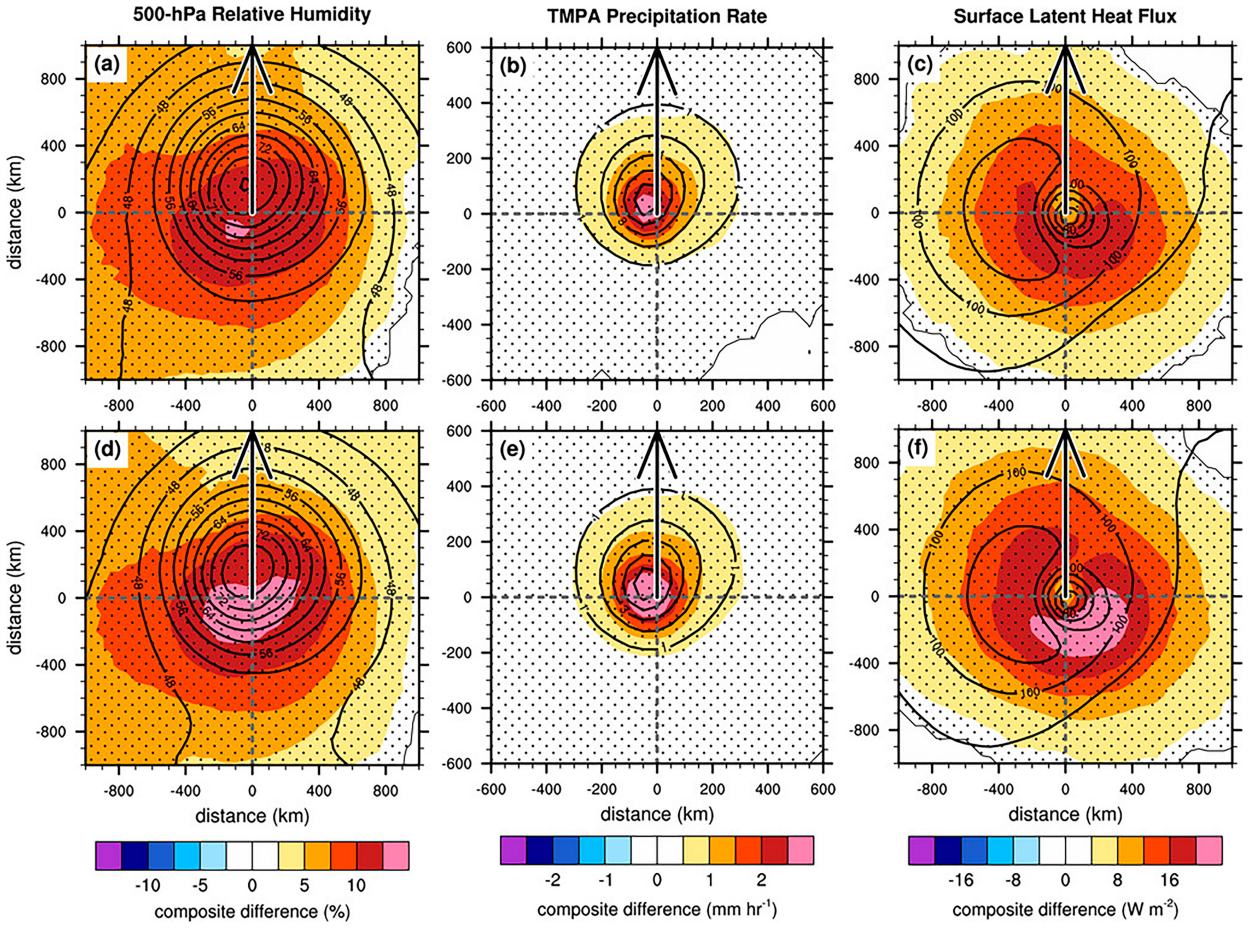

FIG. 12. Storm-centered, shear-relative analyses of (a),(d) 500 hPa RH (%), (b),(e) precipitation rate (mm h^{-1}), and (c),(f) surface latent heat flux (W m^{-2}) at (top) 0 h and (bottom) averaged between 0 and 24 h. Black contours represent the mean of all intensifying and steady-state events, shading represents the composite difference between intensifying and steady-state events, and the stippling pattern represents statistically significant differences at the 99.9% confidence level. All fields were rotated with respect to the 200–850 hPa shear vector such that the shear vector (black and white arrow) points along the positive ordinate [from Fig. 11 in Rios-Berrios and Torn (2017)].

increase in stratiform precipitation may be linked to a moistening of the inner core, promoting a local thermodynamic environment that favors more axisymmetric heating during rapid intensification. This hypothesis is consistent with a comparison of steady-state and intensifying TCs in the presence of moderate VWS by Rios-Berrios and Torn (2017), who found intensifying TCs have a more humid midtroposphere and a greater coverage of upshear precipitation (Fig. 12). Composite analyses from other observational platforms, such as geostationary satellite imagery (Fischer et al. 2018; Shi and Chen 2021), airborne Doppler radar analyses (Rogers et al. 2013; Wadler et al. 2018), and global lightning detection networks (Stevenson et al. 2018), have also emphasized the importance of greater convective axisymmetry for increased rates of TC intensification.

Full-physics numerical simulations similarly point toward the significance of greater precipitation axisymmetry for increased rates of TC intensification in environments with VWS (e.g., Miyamoto and Takemi 2013; Rios-Berrios et al. 2016b; Onderlinde and Nolan 2016; X. Chen et al. 2018a; Leighton et al. 2018; Miyamoto and Nolan 2018; Tao and Zhang 2019; Alvey et al. 2020; Hazelton et al. 2020; Alland et al. 2021b). Analyses of such simulations have inspired hypotheses to explain the increased precipitation axisymmetry of sheared TCs. Some studies have suggested the significance of vortex alignment in facilitating more axisymmetric precipitation structures (e.g., Tao and Zhang 2014; X. Chen et al. 2018b; Rios-Berrios et al. 2018; Ryglicki et al. 2018b; Tao and Zhang 2019; Alvey et al. 2020; Hazelton et al. 2020; Rios-Berrios 2020; Alland et al. 2021b; X. Chen et al. 2021). As discussed in the previous subsection, vortex tilt and asymmetric convection are strongly coupled to each other and, consequently, a nearly aligned vortex is also associated with a more axisymmetric distribution of precipitation. Other studies have emphasized the important role of the boundary layer in facilitating precipitation axisymmetry. In a comparison of two simulations of the same TC vortex over different SSTs, X. Chen et al. (2021) demonstrated how enhanced surface enthalpy fluxes—in this case from warmer sea surface temperatures—promoted more vigorous inner-core convection that propagated farther upshear, leading to greater

precipitation axisymmetry and increased TC intensification rates. Likewise, dropsonde observations (Nguyen et al. 2019), reanalysis output (Rios-Berrios and Torn 2017; Richardson et al. 2022), and other numerical simulations (Rappin and Nolan 2012) generally agree that larger upshear surface enthalpy fluxes favor increased precipitation axisymmetry and subsequent TC intensification.

d. *Outflow blocking*

The divergent upper-level outflow of a TC can in some cases counteract storm-relative flows due to VWS, enabling TCs to intensify in shear. Black and Anthes (1971) recognized the ability of the TC outflow to deflect the upper-tropospheric flow in which the TC is embedded, but more recent work has revealed the implications of this flow deflection for the intensification of sheared TCs. Ryglicki et al. (2018a) identified a class of storms that undergo rapid intensification in moderate to strong deep-layer VWS. A common feature of these storms is that they all exhibit bursts of convection that increase the component of outflow directed upshear, which tends to occur once the vortex tilts to the left of shear (Ryglicki et al. 2020).

Outflow blocking promotes the intensification of sheared TCs by rerouting the environmental flow away from the TC center (Ryglicki et al. 2019, 2021). This reduces the radial thermodynamic ventilation of the warm core in the upper troposphere (Finocchio and Rios-Berrios 2021) and locally reduces the effective wind shear over the TC inner core (Dai et al. 2021). In a composite analysis of several TCs in the Northern Hemisphere, Shi and Chen (2021) found that, consistent with Ryglicki et al. (2020), rapid intensification in moderate to strong shear is preceded by an increase in the component of outflow directed upshear and a coincident reduction of the total shear near the TC inner core. Idealized simulations have identified an asymmetric divergent flow within the outflow layer of sheared TCs that is responsible for locally reducing the vertical wind shear over the inner core (Xu and Wang 2013; Ryglicki et al. 2019; Dai et al. 2021). Because the TC outflow is confined to the upper troposphere, the asymmetric divergent flow is more effective at counteracting VWS that is also concentrated in the upper troposphere (Elsberry and Jeffries 1996; Ryglicki et al. 2018b; Shi and Chen 2021). As discussed in section 3a, upper-level anticyclones are usually responsible for these types of upper-level shear environments (Ryglicki et al. 2018a). Shi and Chen (2021) found that 76% of TCs that rapidly intensify in moderate to strong shear are sheared by an upper-level anticyclone, indicating a possible relationship between the large-scale shearing mechanism and the likelihood for the outflow to counteract VWS. From an operational forecasting perspective, such relationships between the large-scale flow and the likelihood for TC intensification in shear are particularly valuable in the moderate VWS environments that are frequently associated with lower TC predictability.

5. Effects of shear on TC predictability

The presence of VWS increases the complexity of interactions between the TC and its surrounding environment that can strongly limit skillful predictions of TC structure and intensity change. Bhatia and Nolan (2013) found that the short-range intensity forecast errors from both the National Hurricane Center and operational statistical and dynamical models at the time were largest for hurricane-strength storms in moderate magnitudes (5–10 m s^{-1}) of deep-layer VWS. This range of VWS magnitudes is near the threshold values that are traditionally used in operational settings to broadly distinguish favorable from unfavorable flow environments. Although operational intensity forecast skill has improved since Bhatia and Nolan (2013), TCs in moderate VWS environments are still widely considered to be less predictable than TCs in weak or strong shear.

Numerous studies over the last several decades have examined how VWS, and in particular moderate VWS, affects both the intrinsic and practical predictability of a TC. Intrinsic predictability refers to "the extent to which prediction is possible if an optimum procedure is used" (Lorenz 2006). Zhang and Tao (2013) studied the intrinsic predictability of weak TCs in shear using idealized ensemble simulations in which they added small, random moisture perturbations in the TC boundary layer of each ensemble member. They found that as the deep-layer VWS magnitude increased, the uncertainty in the timing of TC intensification increased until the shear became strong enough to prevent intensification in any of the ensemble members (Fig. 13). Tao and Zhang (2015) further explored this result and found that the large ensemble spread in RI onset times of the moderately sheared TCs was attributed to moist convection. The chaotic nature of moist convection introduces small-scale differences among the ensemble members which grow up to the vortex scale as the TCs precess through the downshear-left quadrant, ultimately resulting in differences in vortex precession rates and the timing of RI onset.

VWS also reduces a TC's practical predictability, which is "the extent to which we ourselves are able to predict by the best-known procedures, either currently or in the foreseeable future" (Lorenz 2006). The presence of VWS heightens the sensitivity of the storm to environmental characteristics that are often poorly observed, such as midlevel humidity. Munsell et al. (2013) studied an ensemble of a sheared Tropical Storm Erika (2009) and showed how large variability in midlevel dry-air intrusions played a key role in increasing the ensemble forecast intensity spread. Rios-Berrios et al. (2016a,b) analyzed ensemble simulations of TC Katia (2011) and Hurricane Ophelia (2011), respectively, and found that the key differences between developing and nondeveloping members related to lower-tropospheric moisture in the right-of-shear quadrant for Katia and midtropospheric moisture in the downshear and left-of-shear quadrants for Ophelia. Uncertainty in the environmental VWS itself also introduces uncertainties into TC intensity forecasts (Emanuel et al. 2004). Both idealized and real TC modeling studies have demonstrated how small variations in the wind profile can lead to bifurcating TC intensity responses that are related to differences in vortex tilt and convective bursts near the radius of maximum winds (Finocchio et al. 2016; Finocchio and Majumdar 2017a; Munsell et al. 2017).

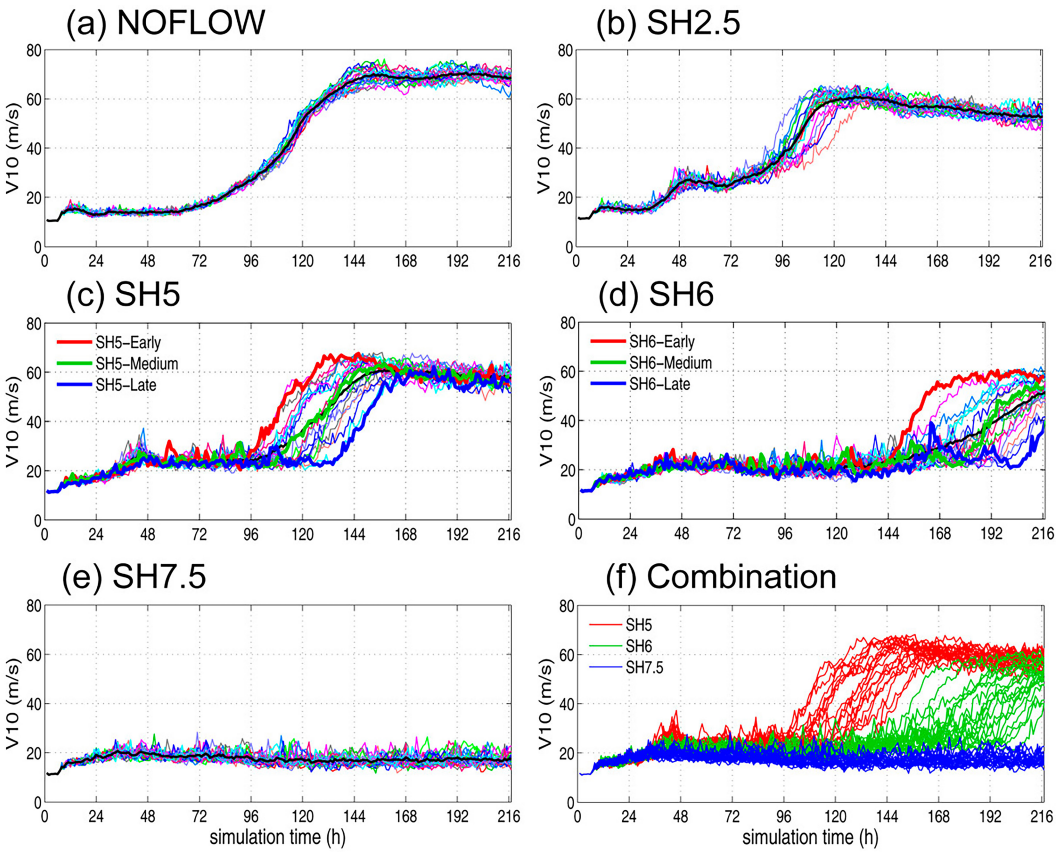

FIG. 13. Time evolution of tropical cyclone intensity in terms of the 10 m maximum wind speed for ensembles with (a) no shear ("NOFLOW"), (b) SH2.5, (c) SH5, (d) SH6, (e) SH7.5, and (f) combination of SH5, SH6, and SH7.5. The numbers after "SH" indicate the magnitude of westerly deep-layer VWS in each ensemble. All simulations have SST = 27°C [adapted from Fig. 2 in Tao and Zhang (2015)].

Other factors related to numerical weather prediction techniques, such as radiation schemes, also influence how VWS affects the practical predictability of a TC. Rios-Berrios (2020) found that using a comprehensive radiation scheme in idealized simulations increases predictability of sheared TCs by stabilizing the lower troposphere, thereby reducing the variability of the nonlinear feedbacks among lower-tropospheric ventilation, cold pools, convection, and vortex tilt. More research is needed on how cloud microphysical parameterizations influence the practical predictability of sheared TCs.

The presence of VWS also affects the structural predictability of a TC through its influence on the evolution of wind, cloud, and precipitation asymmetries. Judt et al. (2016) examined TC structural predictability by azimuthally decomposing the tangential wind field of Hurricane Earl (2010). The mean vortex and wavenumber-1 asymmetry had the longest intrinsic predictability of at least seven days. Notably, they found that the predictability of the mean vortex and wavenumber-1 asymmetry was strongly influenced by the predictability of the environmental deep-layer VWS, which itself remains predictable for longer than a week (Komaromi and Majumdar 2014, 2015). At the scales of individual convective cells (azimuthal wavenumbers > 20), however, errors grow more rapidly in both magnitude and scale, resulting in a much shorter predictability horizon of only 6–12 h (Judt et al. 2016). Similar to the tangential winds, the low-wavenumber asymmetries of the precipitation structure of a sheared TC remain predictable longer than the convective-scale asymmetries (Finocchio and Majumdar 2017a). Moderate shear environments are generally associated with lower intrinsic predictability of TC structure due to heightened sensitivity to the environmental wind profile (Finocchio and Majumdar 2017a), and a higher uncertainty in the vortex tilt evolution (Tao and Zhang 2015; Yu et al. 2023) and the occurrence of eyewall replacement cycles (Zhang et al. 2017).

6. Conclusions and recommendations

Deep-layer VWS, broadly defined as the 200–850 hPa shear of the horizontal wind, has profound effects on TC structure and intensity. This review article summarizes the growing body of research into those effects in terms of their influence on the likelihood and timing of TC intensification. VWS tilts the TC vortex, organizes precipitation into a wavenumber-1 asymmetric pattern, and causes thermal and kinematic asymmetries. While VWS is a useful metric for TC intensity

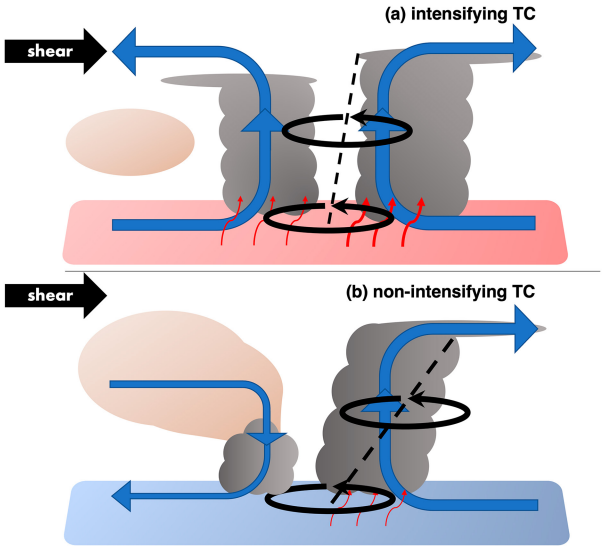

FIG. 14. Summary schematics of key structural properties of (a) intensifying and (b) nonintensifying TCs under moderate VWS. The intensifying TC is associated with nearly symmetric convection (represented by the clouds), a relatively small vortex tilt (represented by the dashed black line), and relatively strong surface fluxes (represented by the small red arrows) in all quadrants. Dry air (represented by the brown circle), if present, is not able to disrupt the TC secondary circulation. The nonintensifying TC is associated with asymmetric convection in the downshear half, a relatively large vortex tilt, and relatively strong surface fluxes in the downshear half. Dry air is able to disrupt the TC through either radial ventilation, downward ventilation, or a combination of both. The intensifying TC is over relatively warmer ocean temperatures than the nonintensifying TC [inspired by schematics from Nguyen et al. (2017), Richardson et al. (2022), and others].

forecasting, recent research demonstrates how shear alone often cannot fully capture the myriad ways in which a TC responds to a given environmental flow. A particularly challenging forecasting situation, which is the focus of several studies reviewed herein, involves an intermediate range of shear magnitudes commonly referred to as moderate shear. Within this range of shear magnitudes, the sensitivity of a TC to subtle aspects of both the storm and its environment are amplified, such that the response of the TC becomes exceedingly difficult to predict.

Several recent studies have identified underlying processes that limit the predictability of moderately sheared TCs. A focus of many of these studies has been on the surprising ability of some TCs to intensify in moderate to strong VWS. Figure 14 shows a summary of the key structural features that distinguish intensifying from nonintensifying TCs under moderate to strong VWS, based on the *existing* knowledge reviewed herein. This review article summarized four different pathways by which a TC can become resilient to such shear environments. Those pathways include the reduction of shear-induced vortex tilt, the formation of a new TC vortex within the shear-organized convection, the transition from a highly asymmetric to nearly symmetric precipitation structure, and the reduction of shear-induced ventilation by outflow blocking (Fig. 14). Several of these pathways operate simultaneously; for example, shear-organized asymmetric convection can lead to the formation of a new, nearly aligned vortex and the associated outflow can counteract the storm-relative inflow due to shear.

Despite the remarkable progress in understanding TC–VWS interactions, many open questions and opportunities for future research remain. There is no widely accepted definition of VWS that can be generally applied in operational and research applications. Some methods estimate VWS by simply taking an area average of the 200 and 850 hPa winds over a large-enough radii (e.g., 500 or 200–800 km) to sample the environment, whereas other methods remove the contributions from the TC vortex before taking such area averages. The specific radii are largely based on legacy from previous studies without physically based justifications. The precise VWS magnitude can vary substantially from one method to another as noted, for example, by Velden and Sears (2014) and Ryglicki et al. (2019, 2021). More broadly, it is unclear how much the calculated shear and other environmental parameters truly affect a TC. For example, does the inner-core vortex of a TC experience the environmental shear that is calculated from a 200–800 km radial average around it? Although the answer to this question will depend on many factors (e.g., TC size, vortex depth), a broadly agreed upon and physically based definition is much needed.

Another research area of opportunity is better understanding the response of early-stage TCs to VWS. Much of the theoretical work on TC intensity and structure is based on the assumption of an axisymmetric vortex; however, early-stage TCs challenge that assumption due to their disorganized and asymmetric nature. For example, how strongly coupled are the displaced circulations of a weak TC in comparison to a vertically tilted vortex of a mature hurricane? Which processes govern the azimuthal distribution and intensity of precipitation of weak TCs? The emerging work on TC intensification under moderate VWS has largely focused on early-stage TCs, but that work has heavily relied on model simulations. Recent advancements in observing platforms (e.g., GOES-R, small satellites, uncrewed aircraft) and increased research flights into early-stage TCs offer potential avenues for expanding our knowledge and aiding theoretical developments applicable to weak and mature TCs alike.

Future studies should continue to interconnect the four pathways discussed here to explain TC intensification under moderate VWS. It is evident that the coupling between circulation and convection is important; however, there are some findings that need clarification. While a recent series of studies emphasizes the role of divergent outflow from shear-induced convection enabling vortex tilt reduction (Ryglicki et al. 2018a,b, 2019, 2020, 2021), other studies focus on boundary layer processes that promote and sustain convection leading to vortex tilt reduction (Rios-Berrios et al. 2018; Rios-Berrios 2020; X. Chen et al. 2021). These processes are not necessarily independent of each other. Hence, more studies are needed to unify these processes.

Many of the studies discussed herein used idealized TC simulations of different complexities, but their numerical configuration could be improved to advance our process-based

understanding of TC–VWS interactions. These simulations usually apply spatially and temporally homogeneous VWS, but Rios-Berrios and Torn (2017) showed that such an assumption is valid for less than 36 h in real-world TCs. New methods to account for the spatial and temporal variability of VWS (e.g., Onderlinde and Nolan 2017) should be used more often to mimic more closely the evolution of observed TCs. Moreover, details of the experimental configuration vary substantially among studies including the specified profile of environmental winds, the choice to introduce shear in the initial conditions or abruptly at some later point in the simulation, the inclusion of warm rain processes alone versus also including ice processes, and the inclusion of radiative processes. This could potentially be alleviated by developing and adopting a generalized configuration. However, details of the simulations will inevitably depend on the underlying model and choices of model parameterizations. To date, all simulations have used convection-permitting or coarser resolution, but large-eddy simulations (LES) remain an area of future research. LES experiments could shed new light on the role of convective processes during TC–VWS interactions; for example, is ventilation a mesoscale process, a turbulent process affecting cloudy updrafts, or both?

Last, there is a critical need for bridging the gap between operational and research efforts. Real-time observational strategies should be informed by the findings of process-based research by developing observational technologies and techniques that sample relevant regions and quantities (such as upshear moisture or boundary layer wind asymmetries). Collocated observations of moisture and winds near ventilation regions could help characterize ventilation in real time. At the same time, future research and forecast product development should be informed by the needs of forecasters given the limited predictability of sheared TCs.

To sum up, we offer the following recommendations for future research on sheared TCs:

- Develop physically based and general methods to diagnose VWS in both operational and research applications.
- Adapt observational strategies and exploit existing observations to better quantify TC–VWS interactions.
- Conduct more research to understand when VWS is detrimental versus beneficial for TC intensity, to further explore the dependency of VWS impacts on TC structure and intensity, and to better interconnect the pathways to intensification under moderate VWS.

Research and operational efforts on the topics above would be highly beneficial for advancing our understanding and improving the prediction of TC formation and intensification.

Acknowledgments. We thank Michael Riemer, Yuqing Wang, David S. Nolan, and two anonymous reviewers for their thoughtful feedback during the peer review process. We also thank Robert F. Rogers, Paul D. Reasor, Joshua H. Cossuth, Daniel P. Stern, and two anonymous reviewers from the National Hurricane Center for providing valuable feedback on an earlier version of this manuscript. This material is based upon work supported by the National Center for Atmospheric Research, which is a major facility sponsored by the National Science Foundation under Cooperative Agreement 1852977. RRB, PF, and MSF also acknowledge funding from the Office of Naval Research under Grants PE 0601153N, N00014-20-1-2071, and ONR-005722, respectively, as part of the Tropical Cyclone Rapid Intensification Departmental Research Initiative.

Data availability statement. No datasets were generated or analyzed during the current study.

REFERENCES

Ahern, K., R. E. Hart, and M. A. Bourassa, 2021: Asymmetric hurricane boundary layer structure during storm decay. Part I: Formation of descending inflow. *Mon. Wea. Rev.*, **149**, 3851–3874, https://doi.org/10.1175/MWR-D-21-0030.1.

Alland, J. J., and C. A. Davis, 2022: Effects of surface fluxes on ventilation pathways and the intensification of Hurricane Michael (2018). *J. Atmos. Sci.*, **79**, 1211–1229, https://doi.org/10.1175/JAS-D-21-0166.1.

——, B. H. Tang, and K. L. Corbosiero, 2017: Effects of midlevel dry air on development of the axisymmetric tropical cyclone secondary circulation. *J. Atmos. Sci.*, **74**, 1455–1470, https://doi.org/10.1175/JAS-D-16-0271.1.

——, ——, ——, and G. H. Bryan, 2021a: Combined effects of midlevel dry air and vertical wind shear on tropical cyclone development. Part I: Downdraft ventilation. *J. Atmos. Sci.*, **78**, 763–782, https://doi.org/10.1175/JAS-D-20-0054.1.

——, ——, ——, and ——, 2021b: Combined effects of midlevel dry air and vertical wind shear on tropical cyclone development. Part II: Radial ventilation. *J. Atmos. Sci.*, **78**, 783–796, https://doi.org/10.1175/JAS-D-20-0055.1.

Alvey, G. R., III, and A. Hazelton, 2022: How do weak, misaligned tropical cyclones evolve toward alignment? A multicase study using the Hurricane Analysis and Forecast System. *J. Geophys. Res. Atmos.*, **127**, e2022JD037268, https://doi.org/10.1029/2022JD037268.

——, J. Zawislak, and E. Zipser, 2015: Precipitation properties observed during tropical cyclone intensity change. *Mon. Wea. Rev.*, **143**, 4476–4492, https://doi.org/10.1175/MWR-D-15-0065.1.

——, E. Zipser, and J. Zawislak, 2020: How does Hurricane Edouard (2014) evolve toward symmetry before rapid intensification? A high-resolution ensemble study. *J. Atmos. Sci.*, **77**, 1329–1351, https://doi.org/10.1175/JAS-D-18-0355.1.

——, M. Fischer, P. Reasor, J. Zawislak, and R. Rogers, 2022: Observed processes underlying the favorable vortex repositioning early in the development of Hurricane Dorian (2019). *Mon. Wea. Rev.*, **150**, 193–213, https://doi.org/10.1175/MWR-D-21-0069.1.

Barnes, G. M., E. J. Zipser, D. Jorgenson, and F. J. Marks Jr., 1983: Mesoscale and convective structure of a hurricane rainband. *J. Atmos. Sci.*, **40**, 2125–2137, https://doi.org/10.1175/1520-0469(1983)040<2125:MACSOA>2.0.CO;2.

Bender, M. A., 1997: The effect of relative flow on the asymmetric structure in the interior of hurricanes. *J. Atmos. Sci.*, **54**, 703–724, https://doi.org/10.1175/1520-0469(1997)054<0703:TEORFO>2.0.CO;2.

Bhatia, K. T., and D. S. Nolan, 2013: Relating the skill of tropical cyclone intensity forecasts to the synoptic environment. *Wea. Forecasting*, **28**, 961–980, https://doi.org/10.1175/WAF-D-12-00110.1.

Bister, M., and K. A. Emanuel, 1997: The genesis of Hurricane Guillermo: TEXMEX analyses and a modeling study. *Mon. Wea. Rev.*, **125**, 2662–2682, https://doi.org/10.1175/1520-0493(1997)125<2662:TGOHGT>2.0.CO;2.

Black, M. L., J. F. Gamache, F. D. Marks, C. E. Samsury, and H. E. Willoughby, 2002: Eastern Pacific Hurricanes Jimena of 1991 and Olivia of 1994: The effect of vertical shear on structure and intensity. *Mon. Wea. Rev.*, **130**, 2291–2312, https://doi.org/10.1175/1520-0493(2002)130<2291:EPHJOA>2.0.CO;2.

Black, P. G., and R. A. Anthes, 1971: On the asymmetric structure of the tropical cyclone outflow layer. *J. Atmos. Sci.*, **28**, 1348–1366, https://doi.org/10.1175/1520-0469(1971)028<1348:OTASOT>2.0.CO;2.

Boehm, A. M., and M. M. Bell, 2021: Retrieved thermodynamic structure of Hurricane Rita (2005) from airborne multi–Doppler radar data. *J. Atmos. Sci.*, **78**, 1583–1605, https://doi.org/10.1175/JAS-D-20-0195.1.

Braun, S. A., M. T. Montgomery, and Z. Pu, 2006: High-resolution simulation of Hurricane Bonnie (1998). Part I: The organization of eyewall vertical motion. *J. Atmos. Sci.*, **63**, 19–42, https://doi.org/10.1175/JAS3598.1.

——, J. A. Sippel, and D. S. Nolan, 2012: The impact of dry midlevel air on hurricane intensity in idealized simulations with no mean flow. *J. Atmos. Sci.*, **69**, 236–257, https://doi.org/10.1175/JAS-D-10-05007.1.

Bukunt, B. P., and G. M. Barnes, 2015: The subtropical jet stream delivers the coup de grace to Hurricane Felicia (2009). *Wea. Forecasting*, **30**, 1039–1049, https://doi.org/10.1175/WAF-D-15-0004.1.

Cecil, D. J., 2007: Satellite-derived rain rates in vertically sheared tropical cyclones. *Geophys. Res. Lett.*, **34**, L02811, https://doi.org/10.1029/2006GL027942.

Chen, B.-F., C. A. Davis, and Y.-H. Kuo, 2018: Effects of low-level flow orientation and vertical shear on the structure and intensity of tropical cyclones. *Mon. Wea. Rev.*, **146**, 2447–2467, https://doi.org/10.1175/MWR-D-17-0379.1.

——, ——, and ——, 2019: An idealized numerical study of shear-relative low-level mean flow on tropical cyclone intensity and size. *J. Atmos. Sci.*, **76**, 2309–2334, https://doi.org/10.1175/JAS-D-18-0315.1.

——, ——, and ——, 2021: Examination of the combined effect of deep-layer vertical shear direction and lower-tropospheric mean flow on tropical cyclone intensity and size based on the ERA5 reanalysis. *Mon. Wea. Rev.*, **149**, 4057–4076, https://doi.org/10.1175/MWR-D-21-0120.1.

Chen, H., and S. G. Gopalakrishnan, 2015: A study on the asymmetric rapid intensification of Hurricane Earl (2010) using the HWRF system. *J. Atmos. Sci.*, **72**, 531–550, https://doi.org/10.1175/JAS-D-14-0097.1.

Chen, S. S., J. A. Knaff, and F. D. Marks Jr., 2006: Effects of vertical wind shear and storm motion on tropical cyclone rainfall asymmetries deduced from TRMM. *Mon. Wea. Rev.*, **134**, 3190–3208, https://doi.org/10.1175/MWR3245.1.

Chen, X., Y. Wang, J. Fang, and M. Xue, 2018a: A numerical study on rapid intensification of Typhoon Vicente (2012) in the South China Sea. Part II: Roles of inner-core processes. *J. Atmos. Sci.*, **75**, 235–255, https://doi.org/10.1175/JAS-D-17-0129.1.

——, M. Xue, and J. Fang, 2018b: Rapid intensification of Typhoon Mujigae (2015) under different sea surface temperatures: Structural changes leading to rapid intensification. *J. Atmos. Sci.*, **75**, 4313–4335, https://doi.org/10.1175/JAS-D-18-0017.1.

——, J. A. Zhang, and F. D. Marks, 2019: A thermodynamic pathway leading to rapid intensification of tropical cyclones in shear. *Geophys. Res. Lett.*, **46**, 9241–9251, https://doi.org/10.1029/2019GL083667.

——, J.-F. Gu, J. A. Zhang, F. D. Marks, R. F. Rogers, and J. J. Cione, 2021: Boundary layer recovery and precipitation symmetrization preceding rapid intensification of tropical cyclones under shear. *J. Atmos. Sci.*, **78**, 1523–1544, https://doi.org/10.1175/JAS-D-20-0252.1.

Corbosiero, K. L., and J. Molinari, 2002: The effects of vertical wind shear on the distribution of convection in tropical cyclones. *Mon. Wea. Rev.*, **130**, 2110–2123, https://doi.org/10.1175/1520-0493(2002)130<2110:TEOVWS>2.0.CO;2.

——, and ——, 2003: The relationship between storm motion, vertical wind shear, and convective asymmetries in tropical cyclones. *J. Atmos. Sci.*, **60**, 366–376, https://doi.org/10.1175/1520-0469(2003)060<0366:TRBSMV>2.0.CO;2.

Cram, T. A., J. Persing, M. T. Montgomery, and S. A. Braun, 2007: A Lagrangian trajectory view on transport and mixing processes between the eye, eyewall, and environment using a high-resolution simulation of Hurricane Bonnie (1998). *J. Atmos. Sci.*, **64**, 1835–1856, https://doi.org/10.1175/JAS3921.1.

Dai, Y., S. J. Majumdar, and D. S. Nolan, 2021: Tropical cyclone resistance to strong environmental shear. *J. Atmos. Sci.*, **78**, 1275–1293, https://doi.org/10.1175/JAS-D-20-0231.1.

Davies-Jones, R., D. Burgess, and M. Foster, 1990: Test of helicity as a tornado forecast parameter. Preprints, *16th Conf. on Severe Local Storms*, Kananskis Park, AB, Canada, Amer. Meteor. Soc., 588–592.

Davis, C. A., and D. A. Ahijevych, 2012: Mesoscale structural evolution of three tropical weather systems observed during PREDICT. *J. Atmos. Sci.*, **69**, 1284–1305, https://doi.org/10.1175/JAS-D-11-0225.1.

——, S. C. Jones, and M. Riemer, 2008: Hurricane vortex dynamics during Atlantic extratropical transition. *J. Atmos. Sci.*, **65**, 714–736, https://doi.org/10.1175/2007JAS2488.1.

DeHart, J. C., R. A. Houze Jr., and R. F. Rogers, 2014: Quadrant distribution of tropical cyclone inner-core kinematics in relation to environmental shear. *J. Atmos. Sci.*, **71**, 2713–2732, https://doi.org/10.1175/JAS-D-13-0298.1.

DeMaria, M., 1996: The effect of vertical shear on tropical cyclone intensity change. *J. Atmos. Sci.*, **53**, 2076–2088, https://doi.org/10.1175/1520-0469(1996)053<2076:TEOVSO>2.0.CO;2.

——, and J. Kaplan, 1994: A Statistical Hurricane Intensity Prediction Scheme (SHIPS) for the Atlantic basin. *Wea. Forecasting*, **9**, 209–220, https://doi.org/10.1175/1520-0434(1994)009<0209:ASHIPS>2.0.CO;2.

——, and ——, 1999: An updated Statistical Hurricane Intensity Prediction Scheme (SHIPS) for the Atlantic and eastern North Pacific basins. *Wea. Forecasting*, **14**, 326–337, https://doi.org/10.1175/1520-0434(1999)014<0326:AUSHIP>2.0.CO;2.

——, M. Mainelli, L. K. Shay, J. A. Knaff, and J. Kaplan, 2005: Further improvements to the Statistical Hurricane Intensity Prediction Scheme (SHIPS). *Wea. Forecasting*, **20**, 531–543, https://doi.org/10.1175/WAF862.1.

Didlake, A. C., Jr., and R. A. Houze Jr., 2009: Convective-scale downdrafts in the principal rainband of Hurricane Katrina

(2005). *Mon. Wea. Rev.*, **137**, 3269–3293, https://doi.org/10.1175/2009MWR2827.1.

——, and ——, 2013: Convective-scale variations in the inner-core rainbands of tropical cyclones. *J. Atmos. Sci.*, **70**, 504–523, https://doi.org/10.1175/JAS-D-12-0134.1.

——, and M. R. Kumjian, 2018: Examining storm asymmetries in Hurricane Irma (2017) using polarimetric radar observations. *Geophys. Res. Lett.*, **45**, 13 513–13 522, https://doi.org/10.1029/2018GL080739.

——, P. D. Reasor, R. F. Rogers, and W.-C. Lee, 2018: Dynamics of the transition from spiral rainbands to a secondary eyewall in Hurricane Earl (2010). *J. Atmos. Sci.*, **75**, 2909–2929, https://doi.org/10.1175/JAS-D-17-0348.1.

Dunion, J. P., 2011: Rewriting the climatology of the tropical North Atlantic and Caribbean Sea atmosphere. *J. Climate*, **24**, 893–908, https://doi.org/10.1175/2010JCLI3496.1.

Elsberry, R. L., and R. A. Jeffries, 1996: Vertical wind shear influences on tropical cyclone formation and intensification during TCM-92 and TCM-93. *Mon. Wea. Rev.*, **124**, 1374–1387, https://doi.org/10.1175/1520-0493(1996)124<1374:VWSIOT>2.0.CO;2.

Emanuel, K. A., 1989: The finite-amplitude nature of tropical cyclogenesis. *J. Atmos. Sci.*, **46**, 3431–3456, https://doi.org/10.1175/1520-0469(1989)046<3431:TFANOT>2.0.CO;2.

——, 2003: Tropical cyclones. *Annu. Rev. Earth Planet. Sci.*, **31**, 75–104, https://doi.org/10.1146/annurev.earth.31.100901.141259.

——, 2018: 100 years of progress in tropical cyclone research. *A Century of Progress in Atmospheric and Related Sciences: Celebrating the American Meteorological Society Centennial*, *Meteor. Monogr.*, No. 59, Amer. Meteor. Soc., https://doi.org/10.1175/AMSMONOGRAPHS-D-18-0016.1.

——, C. DesAutels, C. Holloway, and R. Korty, 2004: Environmental control of tropical cyclone intensity. *J. Atmos. Sci.*, **61**, 843–858, https://doi.org/10.1175/1520-0469(2004)061<0843:ECOTCI>2.0.CO;2.

Feng, Y.-C., and M. M. Bell, 2019: Microphysical characteristics of an asymmetric eyewall in major Hurricane Harvey (2017). *Geophys. Res. Lett.*, **46**, 461–471, https://doi.org/10.1029/2018GL080770.

Finocchio, P. M., and S. J. Majumdar, 2017a: The predictability of idealized tropical cyclones in environments with time-varying vertical wind shear. *J. Adv. Model. Earth Syst.*, **9**, 2836–2862, https://doi.org/10.1002/2017MS001168.

——, and ——, 2017b: A statistical perspective on wind profiles and vertical wind shear in tropical cyclone environments of the Northern Hemisphere. *Mon. Wea. Rev.*, **145**, 361–378, https://doi.org/10.1175/MWR-D-16-0221.1.

——, and R. Rios-Berrios, 2021: The intensity- and size-dependent response of tropical cyclones to increasing vertical wind shear. *J. Atmos. Sci*, **78**, 3673–3690, https://doi.org/10.1175/JAS-D-21-0126.1.

——, S. J. Majumdar, D. S. Nolan, and M. Iskandarani, 2016: Idealized tropical cyclone responses to the height and depth of environmental vertical wind shear. *Mon. Wea. Rev.*, **144**, 2155–2175, https://doi.org/10.1175/MWR-D-15-0320.1.

Fischer, M. S., B. H. Tang, K. L. Corbosiero, and C. M. Rozoff, 2018: Normalized convective characteristics of tropical cyclone rapid intensification events in the North Atlantic and eastern North Pacific. *Mon. Wea. Rev.*, **146**, 1133–1155, https://doi.org/10.1175/MWR-D-17-0239.1.

——, P. D. Reasor, R. F. Rogers, and J. F. Gamache, 2022: An analysis of tropical cyclone vortex and convective characteristics in relation to storm intensity using a novel airborne Doppler radar database. *Mon. Wea. Rev.*, **150**, 2255–2278, https://doi.org/10.1175/MWR-D-21-0223.1.

——, ——, B. H. Tang, K. L. Corbosiero, R. D. Torn, and X. Chen, 2023: A tale of two vortex evolutions: Using a high-resolution ensemble to assess the impacts of ventilation on a tropical cyclone rapid intensification event. *Mon. Wea. Rev.*, **151**, 297–320, https://doi.org/10.1175/MWR-D-22-0037.1.

——, R. F. Rogers, P. D. Reasor, and J. P. Dunion, 2024: An observational analysis of the relationship between tropical cyclone vortex tilt, precipitation structure, and intensity change. *Mon. Wea. Rev.*, **152**, 203–225, https://doi.org/10.1175/MWR-D-23-0089.1.

Flatau, M., W. H. Schubert, and D. E. Stevens, 1994: The role of baroclinic processes in tropical cyclone motion: The influence of vertical tilt. *J. Atmos. Sci.*, **51**, 2589–2601, https://doi.org/10.1175/1520-0469(1994)051<2589:TROBPI>2.0.CO;2.

Foerster, A. M., M. M. Bell, P. A. Harr, and S. C. Jones, 2014: Observations of the eyewall structure of Typhoon Sinlaku (2008) during the transformation stage of extratropical transition. *Mon. Wea. Rev.*, **142**, 3372–3392, https://doi.org/10.1175/MWR-D-13-00313.1.

Frank, W. M., and E. A. Ritchie, 1999: Effects of environmental flow upon tropical cyclone structure. *Mon. Wea. Rev.*, **127**, 2044–2061, https://doi.org/10.1175/1520-0493(1999)127<2044:EOEFUT>2.0.CO;2.

——, and ——, 2001: Effects of vertical wind shear on the intensity and structure of numerically simulated hurricanes. *Mon. Wea. Rev.*, **129**, 2249–2269, https://doi.org/10.1175/1520-0493(2001)129<2249:EOVWSO>2.0.CO;2.

Fu, H., Y. Wang, M. Riemer, and Q. Li, 2019: Effect of unidirectional vertical wind shear on tropical cyclone intensity change—Lower-layer shear versus upper-layer shear. *J. Geophys. Res. Atmos.*, **124**, 6265–6282, https://doi.org/10.1029/2019JD030586.

Galarneau, T. J., Jr., and C. A. Davis, 2013: Diagnosing forecast errors in tropical cyclone motion. *Mon. Wea. Rev.*, **141**, 405–430, https://doi.org/10.1175/MWR-D-12-00071.1.

Gao, S., S. Zhai, B. Chen, and T. Li, 2017: Water budget and intensity change of tropical cyclones over the western North Pacific. *Mon. Wea. Rev.*, **145**, 3009–3023, https://doi.org/10.1175/MWR-D-17-0033.1.

Ge, X., T. Li, and M. Peng, 2013: Effects of vertical shears and midlevel dry air on tropical cyclone developments. *J. Atmos. Sci.*, **70**, 3859–3875, https://doi.org/10.1175/JAS-D-13-066.1.

Gray, W. M., 1968: Global view of the origin of tropical disturbances and storms. *Mon. Wea. Rev.*, **96**, 669–700, https://doi.org/10.1175/1520-0493(1968)096<0669:GVOTOO>2.0.CO;2.

Gu, J.-F., Z.-M. Tan, and X. Qiu, 2016: Quadrant-dependent evolution of low-level tangential wind of a tropical cyclone in the shear flow. *J. Atmos. Sci.*, **73**, 1159–1177, https://doi.org/10.1175/JAS-D-15-0165.1.

——, ——, and ——, 2018: The evolution of vortex tilt and vertical motion of tropical cyclones in directional shear flows. *J. Atmos. Sci.*, **75**, 3565–3578, https://doi.org/10.1175/JAS-D-18-0024.1.

——, ——, and ——, 2019: Intensification variability of tropical cyclones in directional shear flows: Vortex tilt–convection coupling. *J. Atmos. Sci.*, **76**, 1827–1844, https://doi.org/10.1175/JAS-D-18-0282.1.

Guimond, S. R., G. M. Heymsfield, and F. J. Turk, 2010: Multiscale observations of Hurricane Dennis (2005): The effects of hot towers on rapid intensification. *J. Atmos. Sci.*, **67**, 633–654, https://doi.org/10.1175/2009JAS3119.1.

——, ——, P. D. Reasor, and A. C. Didlake Jr., 2016: The rapid intensification of Hurricane Karl (2010): New remote sensing observations of convective bursts from the Global Hawk platform. *J. Atmos. Sci.*, **73**, 3617–3639, https://doi.org/10.1175/JAS-D-16-0026.1.

Harnos, D. S., and S. W. Nesbitt, 2011: Convective structure in rapidly intensifying tropical cyclones as depicted by passive microwave measurements. *Geophys. Res. Lett.*, **38**, L07805, https://doi.org/10.1029/2011GL047010.

——, and ——, 2016: Passive microwave quantification of tropical cyclone inner-core cloud populations relative to subsequent intensity change. *Mon. Wea. Rev.*, **144**, 4461–4482, https://doi.org/10.1175/MWR-D-15-0090.1.

Hazelton, A. T., R. E. Hart, and R. F. Rogers, 2017: Analyzing simulated convective bursts in two Atlantic hurricanes. Part II: Intensity change due to bursts. *Mon. Wea. Rev.*, **145**, 3095–3117, https://doi.org/10.1175/MWR-D-16-0268.1.

——, X. Zhang, S. Gopalakrishnan, W. Ramstrom, F. Marks, and J. A. Zhang, 2020: High-resolution ensemble HFV3 forecasts of Hurricane Michael (2018): Rapid intensification in shear. *Mon. Wea. Rev.*, **148**, 2009–2032, https://doi.org/10.1175/MWR-D-19-0275.1.

Helms, C. N., and R. E. Hart, 2015: The evolution of dropsonde-derived kinematic and thermodynamic structures in developing and nondeveloping Atlantic tropical convective systems. *Mon. Wea. Rev.*, **143**, 3109–3135, https://doi.org/10.1175/MWR-D-14-00242.1.

Hence, D. A., and R. A. Houze Jr., 2008: Kinematic structure of convective-scale elements in the rainbands of Hurricanes Katrina and Rita (2005). *J. Geophys. Res.*, **113**, D15108, https://doi.org/10.1029/2007JD009429.

——, and ——, 2011: Vertical structure of hurricane eyewalls as seen by the TRMM Precipitation Radar. *J. Atmos. Sci.*, **68**, 1637–1652, https://doi.org/10.1175/2011JAS3578.1.

Hendricks, E. A., M. T. Montgomery, and C. A. Davis, 2004: The role of "vortical" hot towers in the formation of Tropical Cyclone Diana (1984). *J. Atmos. Sci.*, **61**, 1209–1232, https://doi.org/10.1175/1520-0469(2004)061<1209:TROVHT>2.0.CO;2.

Heymsfield, G. M., J. B. Halverson, J. Simpson, L. Tian, and T. P. Bui, 2001: ER-2 Doppler radar investigations of the eyewall of Hurricane Bonnie during the Convection and Moisture Experiment-3. *J. Appl. Meteor.*, **40**, 1310–1330, https://doi.org/10.1175/1520-0450(2001)040<1310:EDRIOT>2.0.CO;2.

Hill, K. A., and G. M. Lackmann, 2009: Influence of environmental humidity on tropical cyclone size. *Mon. Wea. Rev.*, **137**, 3294–3315, https://doi.org/10.1175/2009MWR2679.1.

Hogsett, W. A., and S. R. Stewart, 2014: Dynamics of tropical cyclone intensification: Deep convective cyclonic "left movers." *J. Atmos. Sci.*, **71**, 226–242, https://doi.org/10.1175/JAS-D-12-0284.1.

Jiang, H., and E. M. Ramirez, 2013: Necessary conditions for tropical cyclone rapid intensification as derived from 11 years of TRMM data. *J. Climate*, **26**, 6459–6470, https://doi.org/10.1175/JCLI-D-12-00432.1.

Jones, S. C., 1995: The evolution of vortices in vertical shear. I: Initially barotropic vortices. *Quart. J. Roy. Meteor. Soc.*, **121**, 821–851, https://doi.org/10.1002/qj.49712152406.

——, 2000a: The evolution of vortices in vertical shear. II: Large-scale asymmetries. *Quart. J. Roy. Meteor. Soc.*, **126**, 3137–3159, https://doi.org/10.1002/qj.49712657008.

——, 2000b: The evolution of vortices in vertical shear. III: Baroclinic vortices. *Quart. J. Roy. Meteor. Soc.*, **126**, 3161–3185, https://doi.org/10.1002/qj.49712657009.

——, 2004: On the ability of dry tropical-cyclone-like vortices to withstand vertical shear. *J. Atmos. Sci.*, **61**, 114–119, https://doi.org/10.1175/1520-0469(2004)061<0114:OTAODT>2.0.CO;2.

Jordan, C. L., 1958: Mean soundings for the West Indies area. *J. Meteor.*, **15**, 91–97, https://doi.org/10.1175/1520-0469(1958)015<0091:MSFTWI>2.0.CO;2.

Judt, F., S. S. Chen, and J. Berner, 2016: Predictability of tropical cyclone intensity: Scale-dependent forecast error growth in high-resolution stochastic kinetic-energy backscatter ensembles. *Quart. J. Roy. Meteor. Soc.*, **142**, 43–57, https://doi.org/10.1002/qj.2626.

Juračić, A., and D. J. Raymond, 2016: The effects of moist entropy and moisture budgets on tropical cyclone development. *J. Geophys. Res. Atmos.*, **121**, 9458–9473, https://doi.org/10.1002/2016JD025065.

Kimball, S. K., 2006: A modeling study of hurricane landfall in a dry environment. *Mon. Wea. Rev.*, **134**, 1901–1918, https://doi.org/10.1175/MWR3155.1.

Komaromi, W. A., 2013: An investigation of composite dropsonde profiles for developing and nondeveloping tropical waves during the 2010 PREDICT field campaign. *J. Atmos. Sci.*, **70**, 542–558, https://doi.org/10.1175/JAS-D-12-052.1.

——, and S. J. Majumdar, 2014: Ensemble-based error and predictability metrics associated with tropical cyclogenesis. Part I: Basinwide perspective. *Mon. Wea. Rev.*, **142**, 2879–2898, https://doi.org/10.1175/MWR-D-13-00370.1.

——, and ——, 2015: Ensemble-based error and predictability metrics associated with tropical cyclogenesis. Part II: Wave-relative framework. *Mon. Wea. Rev.*, **143**, 1665–1686, https://doi.org/10.1175/MWR-D-14-00286.1.

Kossin, J. P., and W. H. Schubert, 2001: Mesovortices, polygonal flow patterns, and rapid pressure falls in hurricane-like vortices. *J. Atmos. Sci.*, **58**, 2196–2209, https://doi.org/10.1175/1520-0469(2001)058<2196:MPFPAR>2.0.CO;2.

Kurihara, Y., M. A. Bender, and R. J. Ross, 1993: An initialization scheme of hurricane models by vortex specification. *Mon. Wea. Rev.*, **121**, 2030–2045, https://doi.org/10.1175/1520-0493(1993)121<2030:AISOHM>2.0.CO;2.

Kwon, Y. C., and W. M. Frank, 2005: Dynamic instabilities of simulated hurricane-like vortices and their impacts on the core structure of hurricanes. Part I: Dry experiments. *J. Atmos. Sci.*, **62**, 3955–3973, https://doi.org/10.1175/JAS3575.1.

——, and ——, 2008: Dynamic instabilities of simulated hurricane-like vortices and their impacts on the core structure of hurricanes. Part II: Moist experiments. *J. Atmos. Sci.*, **65**, 106–122, https://doi.org/10.1175/2007JAS2132.1.

Laurencin, C. N., A. C. Didlake Jr., S. D. Loeffler, M. R. Kumjian, and G. M. Heymsfield, 2020: Hydrometeor size sorting in the asymmetric eyewall of Hurricane Matthew (2016). *J. Geophys. Res. Atmos.*, **125**, e2020JD032671, https://doi.org/10.1029/2020JD032671.

Lee, T.-Y., C.-C. Wu, and R. Rios-Berrios, 2021: The role of low-level flow direction on tropical cyclone intensity changes in a moderate-sheared environment. *J. Atmos. Sci.*, **78**, 2859–2877, https://doi.org/10.1175/JAS-D-20-0360.1.

Leighton, H., S. Gopalakrishnan, J. A. Zhang, R. F. Rogers, Z. Zhang, and V. Tallapragada, 2018: Azimuthal distribution of deep convection, environmental factors, and tropical cyclone rapid intensification: A perspective from HWRF ensemble forecasts of Hurricane Edouard (2014). *J. Atmos. Sci.*, **75**, 275–295, https://doi.org/10.1175/JAS-D-17-0171.1.

Lonfat, M., F. D. Marks Jr., and S. S. Chen, 2004: Precipitation distribution in tropical cyclones using the Tropical Rainfall

Measuring Mission (TRMM) Microwave Imager: A global perspective. *Mon. Wea. Rev.*, **132**, 1645–1660, https://doi.org/10.1175/1520-0493(2004)132<1645:PDITCU>2.0.CO;2.

——, R. Rogers, T. Marchok, and F. D. Marks Jr., 2007: A parametric model for predicting hurricane rainfall. *Mon. Wea. Rev.*, **135**, 3086–3097, https://doi.org/10.1175/MWR3433.1.

López, R. E., 1968: Investigation of the importance of cumulus convection and ventilation in early tropical storm development. Colorado State University Atmospheric Sciences Tech. Paper 124, 88 pp.

Lorenz, E. N., 2006: Predictability—A problem partly solved. *Predictability of Weather and Climate*, T. Palmer and R. Hagedorn, Eds., Cambridge University Press, 40–58, https://doi.org/10.1017/CBO9780511617652.004.

Lu, P., N. Lin, K. Emanuel, D. Chavas, and J. Smith, 2018: Assessing hurricane rainfall mechanisms using a physics-based model: Hurricanes Isabel (2003) and Irene (2011). *J. Atmos. Sci.*, **75**, 2337–2358, https://doi.org/10.1175/JAS-D-17-0264.1.

Marks, F. D., Jr., R. A. Houze Jr., and J. F. Gamache, 1992: Dual-aircraft investigation of the inner core of Hurricane Norbert. Part I: Kinematic structure. *J. Atmos. Sci.*, **49**, 919–942, https://doi.org/10.1175/1520-0469(1992)049<0919:DAIOTI>2.0.CO;2.

McBride, J. L., and R. Zehr, 1981: Observational analysis of tropical cyclone formation. Part II: Comparison of non-developing versus developing systems. *J. Atmos. Sci.*, **38**, 1132–1151, https://doi.org/10.1175/1520-0469(1981)038<1132:OAOTCF>2.0.CO;2.

Merrill, R. T., 1988: Environmental influences on hurricane intensification. *J. Atmos. Sci.*, **45**, 1678–1687, https://doi.org/10.1175/1520-0469(1988)045<1678:EIOHI>2.0.CO;2.

Miyamoto, Y., and T. Takemi, 2013: A transition mechanism for the spontaneous axisymmetric intensification of tropical cyclones. *J. Atmos. Sci.*, **70**, 112–129, https://doi.org/10.1175/JAS-D-11-0285.1.

——, and D. S. Nolan, 2018: Structural changes preceding rapid intensification in tropical cyclones as shown in a large ensemble of idealized simulations. *J. Atmos. Sci.*, **75**, 555–569, https://doi.org/10.1175/JAS-D-17-0177.1.

Molinari, J., and D. Vollaro, 2010: Rapid intensification of a sheared tropical storm. *Mon. Wea. Rev.*, **138**, 3869–3885, https://doi.org/10.1175/2010MWR3378.1.

——, ——, and K. L. Corbosiero, 2004: Tropical cyclone formation in a sheared environment: A case study. *J. Atmos. Sci.*, **61**, 2493–2509, https://doi.org/10.1175/JAS3291.1.

——, P. Dodge, D. Vollaro, K. L. Corbosiero, and F. Marks Jr., 2006: Mesoscale aspects of the downshear reformation of a tropical cyclone. *J. Atmos. Sci.*, **63**, 341–354, https://doi.org/10.1175/JAS3591.1.

——, J. Frank, and D. Vollaro, 2013: Convective bursts, downdraft cooling, and boundary layer recovery in a sheared tropical storm. *Mon. Wea. Rev.*, **141**, 1048–1060, https://doi.org/10.1175/MWR-D-12-00135.1.

Möller, J. D., and M. T. Montgomery, 2000: Tropical cyclone evolution via potential vorticity anomalies in a three-dimensional balance model. *J. Atmos. Sci.*, **57**, 3366–3387, https://doi.org/10.1175/1520-0469(2000)057<3366:TCEVPV>2.0.CO;2.

Montgomery, M. T., and R. K. Smith, 2014: Paradigms for tropical cyclone intensification. *Aust. Meteor. Oceanogr. J.*, **64**, 37–66, https://doi.org/10.22499/2.6401.005.

——, and ——, 2017: Recent developments in the fluid dynamics of tropical cyclones. *Annu. Rev. Fluid Mech.*, **49**, 541–574, https://doi.org/10.1146/annurev-fluid-010816-060022.

——, L. L. Lussier III, R. W. Moore, and Z. Wang, 2010: The genesis of Typhoon Nuri as observed during the Tropical Cyclone Structure 2008 (TCS-08) field experiment. Part 1: The role of the easterly wave critical layer. *Atmos. Chem. Phys.*, **10**, 9879–9900, https://doi.org/10.5194/acp-10-9879-2010.

Munsell, E. B., F. Zhang, and D. P. Stern, 2013: Predictability and dynamics of a nonintensifying tropical storm: Erika (2009). *J. Atmos. Sci.*, **70**, 2505–2524, https://doi.org/10.1175/JAS-D-12-0243.1.

——, ——, J. A. Sippel, S. A. Braun, and Y. Weng, 2017: Dynamics and predictability of the intensification of Hurricane Edouard (2014). *J. Atmos. Sci.*, **74**, 573–595, https://doi.org/10.1175/JAS-D-16-0018.1.

——, S. A. Braun, and F. Zhang, 2021: *GOES-16* observations of rapidly intensifying tropical cyclones: Hurricanes Harvey (2017), Maria (2017), and Michael (2018). *Mon. Wea. Rev*, **149**, 1695–1714, https://doi.org/10.1175/MWR-D-19-0298.1.

Nam, C. C., and M. M. Bell, 2021: Multiscale shear impacts during the genesis of Hagupit (2008). *Mon. Wea. Rev.*, **149**, 551–569, https://doi.org/10.1175/MWR-D-20-0133.1.

——, ——, and D. Tao, 2023: Bifurcation points for tropical cyclone genesis and intensification in sheared and dry environments. *J. Atmos. Sci.*, **80**, 2239–2259, https://doi.org/10.1175/JAS-D-22-0100.1.

Nguyen, L. T., and J. Molinari, 2012: Rapid intensification of a sheared, fast-moving hurricane over the Gulf Stream. *Mon. Wea. Rev.*, **140**, 3361–3378, https://doi.org/10.1175/MWR-D-11-00293.1.

——, and ——, 2015: Simulation of the downshear reformation of a tropical cyclone. *J. Atmos. Sci.*, **72**, 4529–4551, https://doi.org/10.1175/JAS-D-15-0036.1.

——, R. F. Rogers, and P. D. Reasor, 2017: Thermodynamic and kinematic influences on precipitation symmetry in sheared tropical cyclones: Bertha and Cristobal (2014). *Mon. Wea. Rev.*, **145**, 4423–4446, https://doi.org/10.1175/MWR-D-17-0073.1.

——, ——, J. Zawislak, and J. A. Zhang, 2019: Assessing the influence of convective downdrafts and surface enthalpy fluxes on tropical cyclone intensity change in moderate vertical wind shear. *Mon. Wea. Rev.*, **147**, 3519–3534, https://doi.org/10.1175/MWR-D-18-0461.1.

Nolan, D. S., 2007: What is the trigger for tropical cyclogenesis? *Aust. Meteor. Mag.*, **56**, 241–266.

——, 2011: Evaluating environmental favorableness for tropical cyclone development with the method of point-downscaling. *J. Adv. Model. Earth Syst.*, **3**, M08001, https://doi.org/10.1029/2011MS000063.

——, and E. D. Rappin, 2008: Increased sensitivity of tropical cyclogenesis to wind shear in higher SST environments. *Geophys. Res. Lett.*, **35**, L14805, https://doi.org/10.1029/2008GL034147.

——, and M. G. McGauley, 2012: Tropical cyclogenesis in wind shear: Climatological relationships and physical processes. *Cyclones: Formation, Triggers and Control*, K. Oouchi and H. Fudeyasu, Eds., Nova Science Publishers, 1–34.

——, Y. Moon, and D. P. Stern, 2007: Tropical cyclone intensification from asymmetric convection: Energetics and efficiency. *J. Atmos. Sci.*, **64**, 3377–3405, https://doi.org/10.1175/JAS3988.1.

Nugent, A. D., and R. Rios-Berrios, 2018: Factors leading to extreme precipitation on Dominica from Tropical Storm Erika (2015). *Mon. Wea. Rev.*, **146**, 525–541, https://doi.org/10.1175/MWR-D-17-0242.1.

Onderlinde, M. J., and D. S. Nolan, 2014: Environmental helicity and its effects on development and intensification of tropical

cyclones. *J. Atmos. Sci.*, **71**, 4308–4320, https://doi.org/10.1175/JAS-D-14-0085.1.

——, and ——, 2016: Tropical cyclone–relative environmental helicity and the pathways to intensification in shear. *J. Atmos. Sci.*, **73**, 869–890, https://doi.org/10.1175/JAS-D-15-0261.1.

——, and ——, 2017: The tropical cyclone response to changing wind shear using the method of time-varying point-downscaling. *J. Adv. Model. Earth Syst.*, **9**, 908–931, https://doi.org/10.1002/2016MS000796.

Ooyama, K., 1969: Numerical simulation of the life cycle of tropical cyclones. *J. Atmos. Sci.*, **26**, 3–40, https://doi.org/10.1175/1520-0469(1969)026<0003:NSOTLC>2.0.CO;2.

Patra, R., 2004: Idealised modeling of tropical cyclones in vertical wind shear: The role of saturated ascent. *26th Conf. on Hurricanes and Tropical Meteorology*, Miami, FL, Amer. Meteor. Soc., 4A.6, https://ams.confex.com/ams/26HURR/techprogram/paper_75586.htm.

Pei, Y., and H. Jiang, 2018: Quantification of precipitation asymmetries of tropical cyclones using 16-year TRMM observations. *J. Geophys. Res. Atmos.*, **123**, 8091–8114, https://doi.org/10.1029/2018JD028545.

Persing, J., and M. T. Montgomery, 2003: Hurricane superintensity. *J. Atmos. Sci.*, **60**, 2349–2371, https://doi.org/10.1175/1520-0469(2003)060<2349:HS>2.0.CO;2.

Powell, M. D., 1990: Boundary layer structure and dynamics in outer hurricane rainbands. Part II: Downdraft modification and mixed layer recovery. *Mon. Wea. Rev.*, **118**, 918–938, https://doi.org/10.1175/1520-0493(1990)118<0918:BLSADI>2.0.CO;2.

Ramage, C. S., 1959: Hurricane development. *J. Meteor.*, **16**, 227–237, https://doi.org/10.1175/1520-0469(1959)016<0227:HD>2.0.CO;2.

Rappin, E. D., and D. S. Nolan, 2012: The effect of vertical shear orientation on tropical cyclogenesis. *Quart. J. Roy. Meteor. Soc.*, **138**, 1035–1054, https://doi.org/10.1002/qj.977.

——, ——, and K. A. Emanuel, 2010: Thermodynamic control of tropical cyclogenesis in environments of radiative-convective equilibrium with shear. *Quart. J. Roy. Meteor. Soc.*, **136**, 1954–1971, https://doi.org/10.1002/qj.706.

Raymond, D. J., C. López-Carrillo, and L. L. Cavazos, 1998: Case-studies of developing east Pacific easterly waves. *Quart. J. Roy. Meteor. Soc.*, **124**, 2005–2034, https://doi.org/10.1002/qj.49712455011.

——, S. L. Sessions, and C. López-Carrillo, 2011: Thermodynamics of tropical cyclogenesis in the northwest Pacific. *J. Geophys. Res.*, **116**, D18101, https://doi.org/10.1029/2011JD015624.

Reasor, P. D., and M. T. Montgomery, 2001: Three-dimensional alignment and corotation of weak, TC-like vortices via linear vortex Rossby waves. *J. Atmos. Sci.*, **58**, 2306–2330, https://doi.org/10.1175/1520-0469(2001)058<2306:TDAACO>2.0.CO;2.

——, and M. D. Eastin, 2012: Rapidly intensifying Hurricane Guillermo (1997). Part II: Resilience in shear. *Mon. Wea. Rev.*, **140**, 425–444, https://doi.org/10.1175/MWR-D-11-00080.1.

——, and M. T. Montgomery, 2015: Evaluation of a heuristic model for tropical cyclone resilience. *J. Atmos. Sci.*, **72**, 1765–1782, https://doi.org/10.1175/JAS-D-14-0318.1.

——, ——, and L. D. Grasso, 2004: A new look at the problem of tropical cyclones in vertical shear flow: Vortex resiliency. *J. Atmos. Sci.*, **61**, 3–22, https://doi.org/10.1175/1520-0469(2004)061<0003:ANLATP>2.0.CO;2.

——, M. D. Eastin, and J. F. Gamache, 2009: Rapidly intensifying Hurricane Guillermo (1997). Part I: Low-wavenumber structure and evolution. *Mon. Wea. Rev.*, **137**, 603–631, https://doi.org/10.1175/2008MWR2487.1.

——, R. Rogers, and S. Lorsolo, 2013: Environmental flow impacts on tropical cyclone structure diagnosed from airborne Doppler radar composites. *Mon. Wea. Rev.*, **141**, 2949–2969, https://doi.org/10.1175/MWR-D-12-00334.1.

Richardson, J. C., R. D. Torn, and B. H. Tang, 2022: An analog comparison between rapidly and slowly intensifying tropical cyclones. *Mon. Wea. Rev.*, **150**, 2139–2156, https://doi.org/10.1175/MWR-D-21-0260.1.

Riehl, H., and R. J. Shafer, 1944: The recurvature of tropical storms. *J. Meteor.*, **1**, 42–54, https://doi.org/10.1175/1520-0469(1944)001<0001:TROTS>2.0.CO;2.

Riemer, M., 2016: Meso-β-scale environment for the stationary band complex of vertically sheared tropical cyclones. *Quart. J. Roy. Meteor. Soc.*, **142**, 2442–2451, https://doi.org/10.1002/qj.2837.

——, and M. T. Montgomery, 2011: Simple kinematic models for the environmental interaction of tropical cyclones in vertical wind shear. *Atmos. Chem. Phys.*, **11**, 9395–9414, https://doi.org/10.5194/acp-11-9395-2011.

——, and F. Laliberté, 2015: Secondary circulation of tropical cyclones in vertical wind shear: Lagrangian diagnostic and pathways of environmental interaction. *J. Atmos. Sci.*, **72**, 3517–3536, https://doi.org/10.1175/JAS-D-14-0350.1.

——, M. T. Montgomery, and M. E. Nicholls, 2010: A new paradigm for intensity modification of tropical cyclones: Thermodynamic impact of vertical wind shear on the inflow layer. *Atmos. Chem. Phys.*, **10**, 3163–3188, https://doi.org/10.5194/acp-10-3163-2010.

——, ——, and ——, 2013: Further examination of the thermodynamic modification of the inflow layer of tropical cyclones by vertical wind shear. *Atmos. Chem. Phys.*, **13**, 327–346, https://doi.org/10.5194/acp-13-327-2013.

Rios-Berrios, R., 2020: Impacts of radiation and cold pools on the intensity and vortex tilt of weak tropical cyclones interacting with vertical wind shear. *J. Atmos. Sci.*, **77**, 669–689, https://doi.org/10.1175/JAS-D-19-0159.1.

——, and R. D. Torn, 2017: Climatological analysis of tropical cyclone intensity changes under moderate vertical wind shear. *Mon. Wea. Rev.*, **145**, 1717–1738, https://doi.org/10.1175/MWR-D-16-0350.1.

——, ——, and C. A. Davis, 2016a: An ensemble approach to investigate tropical cyclone intensification in sheared environments. Part I: Katia (2011). *J. Atmos. Sci.*, **73**, 71–93, https://doi.org/10.1175/JAS-D-15-0052.1.

——, ——, and ——, 2016b: An ensemble approach to investigate tropical cyclone intensification in sheared environments. Part II: Ophelia (2011). *J. Atmos. Sci.*, **73**, 1555–1575, https://doi.org/10.1175/JAS-D-15-0245.1.

——, C. A. Davis, and R. D. Torn, 2018: A hypothesis for the intensification of tropical cyclones under moderate vertical wind shear. *J. Atmos. Sci.*, **75**, 4149–4173, https://doi.org/10.1175/JAS-D-18-0070.1.

Ritchie, E. A., and W. M. Frank, 2007: Interactions between simulated tropical cyclones and an environment with a variable Coriolis parameter. *Mon. Wea. Rev.*, **135**, 1889–1905, https://doi.org/10.1175/MWR3359.1.

Rivera-Torres, N. G., K. L. Corbosiero, and B. H. Tang, 2023: Factors associated with the downshear reformation of tropical cyclones. *Mon. Wea. Rev.*, **151**, 2717–2737, https://doi.org/10.1175/MWR-D-22-0251.1.

Rogers, R., S. Chen, J. Tenerelli, and H. Willoughby, 2003: A numerical study of the impact of vertical shear on the distribution of rainfall in Hurricane Bonnie (1998). *Mon. Wea. Rev.*, **131**, 1577–1599, https://doi.org/10.1175//2546.1.

——, P. Reasor, and S. Lorsolo, 2013: Airborne Doppler observations of the inner-core structural differences between intensifying and steady-state tropical cyclones. *Mon. Wea. Rev.*, **141**, 2970–2991, https://doi.org/10.1175/MWR-D-12-00357.1.

——, ——, and J. A. Zhang, 2015: Multiscale structure and evolution of Hurricane Earl (2010) during rapid intensification. *Mon. Wea. Rev.*, **143**, 536–562, https://doi.org/10.1175/MWR-D-14-00175.1.

——, J. A. Zhang, J. Zawislak, H. Jiang, G. R. Alvey III, E. J. Zipser, and S. N. Stevenson, 2016: Observations of the structure and evolution of Hurricane Edouard (2014) during intensity change. Part II: Kinematic structure and the distribution of deep convection. *Mon. Wea. Rev.*, **144**, 3355–3376, https://doi.org/10.1175/MWR-D-16-0017.1.

——, P. D. Reasor, J. A. Zawislak, and L. T. Nguyen, 2020: Precipitation processes and vortex alignment during the intensification of a weak tropical cyclone in moderate vertical shear. *Mon. Wea. Rev.*, **148**, 1899–1929, https://doi.org/10.1175/MWR-D-19-0315.1.

Rozoff, C. M., J. P. Kossin, W. H. Schubert, and P. J. Mulero, 2009: Internal control of hurricane intensity variability: The dual nature of potential vorticity mixing. *J. Atmos. Sci.*, **66**, 133–147, https://doi.org/10.1175/2008JAS2717.1.

Ryglicki, D. R., J. H. Cossuth, D. Hodyss, and J. D. Doyle, 2018a: The unexpected rapid intensification of tropical cyclones in moderate vertical wind shear. Part I: Overview and observations. *Mon. Wea. Rev.*, **146**, 3773–3800, https://doi.org/10.1175/MWR-D-18-0020.1.

——, J. D. Doyle, Y. Jin, D. Hodyss, and J. H. Cossuth, 2018b: The unexpected rapid intensification of tropical cyclones in moderate vertical wind shear. Part II: Vortex tilt. *Mon. Wea. Rev.*, **146**, 3801–3825, https://doi.org/10.1175/MWR-D-18-0021.1.

——, ——, D. Hodyss, J. H. Cossuth, Y. Jin, K. C. Viner, and J. M. Schmidt, 2019: The unexpected rapid intensification of tropical cyclones in moderate vertical wind shear. Part III: Outflow–environment interaction. *Mon. Wea. Rev.*, **147**, 2919–2940, https://doi.org/10.1175/MWR-D-18-0370.1.

——, D. Hodyss, and G. Rainwater, 2020: The tropical cyclone as a divergent source in a background flow. *J. Atmos. Sci.*, **77**, 4189–4210, https://doi.org/10.1175/JAS-D-20-0030.1.

——, C. S. Velden, P. D. Reasor, D. Hodyss, and J. D. Doyle, 2021: Observations of atypical rapid intensification characteristics in Hurricane Dorian (2019). *Mon. Wea. Rev*, **149**, 2131–2150, https://doi.org/10.1175/MWR-D-20-0413.1.

Schecter, D. A., 2020: Distinct intensification pathways for a shallow-water vortex subjected to asymmetric "diabatic" forcing. *Dyn. Atmos. Oceans*, **91**, 101156, https://doi.org/10.1016/j.dynatmoce.2020.101156.

——, 2022: Intensification of tilted tropical cyclones over relatively cool and warm oceans in idealized numerical simulations. *J. Atmos. Sci.*, **79**, 485–512, https://doi.org/10.1175/JAS-D-21-0051.1.

——, and M. T. Montgomery, 2003: On the symmetrization rate of an intense geophysical vortex. *Dyn. Atmos. Oceans*, **37**, 55–88, https://doi.org/10.1016/S0377-0265(03)00015-0.

——, and ——, 2007: Waves in a cloudy vortex. *J. Atmos. Sci.*, **64**, 314–337, https://doi.org/10.1175/JAS3849.1.

——, and K. Menelaou, 2020: Development of a misaligned tropical cyclone. *J. Atmos. Sci.*, **77**, 79–111, https://doi.org/10.1175/JAS-D-19-0074.1.

——, M. T. Montgomery, and P. D. Reasor, 2002: A theory for the vertical alignment of a quasigeostrophic vortex. *J. Atmos. Sci.*, **59**, 150–168, https://doi.org/10.1175/1520-0469(2002)059<0150:ATFTVA>2.0.CO;2.

Schubert, W. H., M. T. Montgomery, R. K. Taft, T. A. Guinn, S. R. Fulton, J. P. Kossin, and J. P. Edwards, 1999: Polygonal eyewalls, asymmetric eye contraction, and potential vorticity mixing in hurricanes. *J. Atmos. Sci.*, **56**, 1197–1223, https://doi.org/10.1175/1520-0469(1999)056<1197:PEAECA>2.0.CO;2.

Shelton, K. L., and J. Molinari, 2009: Life of a six-hour hurricane. *Mon. Wea. Rev.*, **137**, 51–67, https://doi.org/10.1175/2008MWR2472.1.

Shi, D., and G. Chen, 2021: The implication of outflow structure for the rapid intensification of tropical cyclones under vertical wind shear. *Mon. Wea. Rev.*, **149**, 4107–4127, https://doi.org/10.1175/MWR-D-21-0141.1.

Shu, S., F. Zhang, J. Ming, and Y. Wang, 2014: Environmental influences on the intensity changes of tropical cyclones over the western North Pacific. *Atmos. Chem. Phys.*, **14**, 6329–6342, https://doi.org/10.5194/acp-14-6329-2014.

Simpson, R., and R. Riehl, 1958: Mid-tropospheric ventilation as a constraint on hurricane development and maintenance. *Tech. Conf. on Hurricanes*, Miami Beach, FL, Amer. Meteor. Soc., D4-1–D4-10.

Smith, R. K., and M. T. Montgomery, 2015: Toward clarity on understanding tropical cyclone intensification. *J. Atmos. Sci.*, **72**, 3020–3031, https://doi.org/10.1175/JAS-D-15-0017.1.

——, W. Ulrich, and G. Sneddon, 2000: On the dynamics of hurricane-like vortices in vertical-shear flows. *Quart. J. Roy. Meteor. Soc.*, **126**, 2653–2670, https://doi.org/10.1002/qj.49712656903.

——, M. T. Montgomery, and N. Van Sang, 2009: Tropical cyclone spin-up revisited. *Quart. J. Roy. Meteor. Soc.*, **135**, 1321–1335, https://doi.org/10.1002/qj.428.

Stevenson, S. N., K. L. Corbosiero, and J. Molinari, 2014: The convective evolution and rapid intensification of Hurricane Earl (2010). *Mon. Wea. Rev.*, **142**, 4364–4380, https://doi.org/10.1175/MWR-D-14-00078.1.

——, ——, and S. F. Abarca, 2016: Lightning in eastern North Pacific tropical cyclones: A comparison to the North Atlantic. *Mon. Wea. Rev.*, **144**, 225–239, https://doi.org/10.1175/MWR-D-15-0276.1.

——, ——, M. DeMaria, and J. L. Vigh, 2018: A 10-year survey of tropical cyclone inner-core lightning bursts and their relationship to intensity change. *Wea. Forecasting*, **33**, 23–36, https://doi.org/10.1175/WAF-D-17-0096.1.

Stone, Ž., G. R. Alvey III, J. P. Dunion, M. S. Fischer, D. J. Raymond, R. F. Rogers, S. Sentic, and J. Zawislak, 2023: Thermodynamic contribution to vortex alignment and rapid intensification of Hurricane Sally (2020). *Mon. Wea. Rev.*, **151**, 931–951, https://doi.org/10.1175/MWR-D-22-0201.1.

Susca-Lopata, G., J. Zawislak, E. J. Zipser, and R. F. Rogers, 2015: The role of observed environmental conditions and precipitation evolution in the rapid intensification of Hurricane Earl (2010). *Mon. Wea. Rev.*, **143**, 2207–2223, https://doi.org/10.1175/MWR-D-14-00283.1.

Tang, B., and K. Emanuel, 2010: Midlevel ventilation's constraint on tropical cyclone intensity. *J. Atmos. Sci.*, **67**, 1817–1830, https://doi.org/10.1175/2010JAS3318.1.

——, and ——, 2012a: Sensitivity of tropical cyclone intensity to ventilation in an axisymmetric model. *J. Atmos. Sci.*, **69**, 2394–2413, https://doi.org/10.1175/JAS-D-11-0232.1.

——, and ——, 2012b: A ventilation index for tropical cyclones. *Bull. Amer. Meteor. Soc.*, **93**, 1901–1912, https://doi.org/10.1175/BAMS-D-11-00165.1.

Tang, X., and F. Zhang, 2016: Impacts of the diurnal radiation cycle on the formation, intensity, and structure of Hurricane Edouard (2014). *J. Atmos. Sci.*, **73**, 2871–2892, https://doi.org/10.1175/JAS-D-15-0283.1.

Tao, C., and H. Jiang, 2015: Distributions of shallow to very deep precipitation–convection in rapidly intensifying tropical cyclones. *J. Climate*, **28**, 8791–8824, https://doi.org/10.1175/JCLI-D-14-00448.1.

——, ——, and J. Zawislak, 2017: The relative importance of stratiform and convective rainfall in rapidly intensifying tropical cyclones. *Mon. Wea. Rev.*, **145**, 795–809, https://doi.org/10.1175/MWR-D-16-0316.1.

Tao, D., and F. Zhang, 2014: Effect of environmental shear, sea-surface temperature, and ambient moisture on the formation and predictability of tropical cyclones: An ensemble-mean perspective. *J. Adv. Model. Earth Syst.*, **6**, 384–404, https://doi.org/10.1002/2014MS000314.

——, and ——, 2015: Effects of vertical wind shear on the predictability of tropical cyclones: Practical versus intrinsic limit. *J. Adv. Model. Earth Syst.*, **7**, 1534–1553, https://doi.org/10.1002/2015MS000474.

——, and ——, 2019: Evolution of dynamic and thermodynamic structures before and during rapid intensification of tropical cyclones: Sensitivity to vertical wind shear. *Mon. Wea. Rev.*, **147**, 1171–1191, https://doi.org/10.1175/MWR-D-18-0173.1.

Tuleya, R. E., and Y. Kurihara, 1981: A numerical study on the effects of environmental flow on tropical storm genesis. *Mon. Wea. Rev.*, **109**, 2487–2506, https://doi.org/10.1175/1520-0493(1981)109<2487:ANSOTE>2.0.CO;2.

Velden, C. S., and J. Sears, 2014: Computing deep-tropospheric vertical wind shear analyses for tropical cyclone applications: Does the methodology matter? *Wea. Forecasting*, **29**, 1169–1180, https://doi.org/10.1175/WAF-D-13-00147.1.

Wadler, J. B., R. F. Rogers, and P. D. Reasor, 2018: The relationship between spatial variations in the structure of convective bursts and tropical cyclone intensification as determined by airborne Doppler radar. *Mon. Wea. Rev.*, **146**, 761–780, https://doi.org/10.1175/MWR-D-17-0213.1.

——, D. S. Nolan, J. A. Zhang, and L. K. Shay, 2021a: Thermodynamic characteristics of downdrafts in tropical cyclones as seen in idealized simulations of different intensities. *J. Atmos. Sci.*, **78**, 3503–3524, https://doi.org/10.1175/JAS-D-21-0006.1.

——, J. A. Zhang, R. F. Rogers, B. Jaimes, and L. K. Shay, 2021b: The rapid intensification of Hurricane Michael (2018): Storm structure and the relationship to environmental and air–sea interactions. *Mon. Wea. Rev.*, **149**, 245–267, https://doi.org/10.1175/MWR-D-20-0145.1.

——, J. J. Cione, J. A. Zhang, E. A. Kalina, and J. Kaplan, 2022: The effects of environmental wind shear direction on tropical cyclone boundary layer thermodynamics and intensity change from multiple observational datasets. *Mon. Wea. Rev.*, **150**, 115–134, https://doi.org/10.1175/MWR-D-21-0022.1.

Wang, C., J. Fang, and Y. Ma, 2022: Structural changes preceding the rapid intensification of Typhoon Lekima (2019) under moderate vertical wind shear. *J. Geophys. Res. Atmos.*, **127**, e2022JD036544, https://doi.org/10.1029/2022JD036544.

Wang, Y., and G. J. Holland, 1996: Tropical cyclone motion and evolution in vertical shear. *J. Atmos. Sci.*, **53**, 3313–3332, https://doi.org/10.1175/1520-0469(1996)053<3313:TCMAEI>2.0.CO;2.

——, and C.-C. Wu, 2004: Current understanding of tropical cyclone structure and intensity changes—A review. *Meteor. Atmos. Phys.*, **87**, 257–278, https://doi.org/10.1007/s00703-003-0055-6.

——, Y. Rao, Z.-M. Tan, and D. Schönemann, 2015: A statistical analysis of the effects of vertical wind shear on tropical cyclone intensity change over the western North Pacific. *Mon. Wea. Rev.*, **143**, 3434–3453, https://doi.org/10.1175/MWR-D-15-0049.1.

Wang, Y.-F., and Z.-M. Tan, 2022: Essential dynamics of the vertical wind shear affecting the secondary eyewall formation in tropical cyclones. *J. Atmos. Sci.*, **79**, 2831–2847, https://doi.org/10.1175/JAS-D-21-0340.1.

Wei, N., X. Zhang, L. Chen, and H. Hu, 2018: Comparison of the effect of easterly and westerly vertical wind shear on tropical cyclone intensity change over the western North Pacific. *Environ. Res. Lett.*, **13**, 034020, https://doi.org/10.1088/1748-9326/aaa496.

Weightman, R. H., 1919: The West India hurricane of September, 1919, in the light of sounding observations. *Mon. Wea. Rev.*, **47**, 717–721, https://doi.org/10.1175/1520-0493(1919)47<717:TWIHOS>2.0.CO;2.

Willoughby, H. E., F. D. Marks Jr., and R. J. Feinberg, 1984: Stationary and moving convective bands in hurricanes. *J. Atmos. Sci.*, **41**, 3189–3211, https://doi.org/10.1175/1520-0469(1984)041<3189:SAMCBI>2.0.CO;2.

Wingo, M. T., and D. J. Cecil, 2010: Effects of vertical wind shear on tropical cyclone precipitation. *Mon. Wea. Rev.*, **138**, 645–662, https://doi.org/10.1175/2009MWR2921.1.

Wong, M. L. M., and J. C. L. Chan, 2004: Tropical cyclone intensity in vertical wind shear. *J. Atmos. Sci.*, **61**, 1859–1876, https://doi.org/10.1175/1520-0469(2004)061<1859:TCIIVW>2.0.CO;2.

Xu, Y., and Y. Wang, 2013: On the initial development of asymmetric vertical motion and horizontal relative flow in a mature tropical cyclone embedded in environmental vertical shear. *J. Atmos. Sci.*, **70**, 3471–3491, https://doi.org/10.1175/JAS-D-12-0335.1.

Yu, C.-L., B. Tang, and R. G. Fovell, 2023: Tropical cyclone tilt and precession in moderate shear: Precession hiatus in a critical shear regime. *J. Atmos. Sci.*, **80**, 909–932, https://doi.org/10.1175/JAS-D-22-0200.1.

Zagrodnik, J. P., and H. Jiang, 2014: Rainfall, convection, and latent heating distributions in rapidly intensifying tropical cyclones. *J. Atmos. Sci.*, **71**, 2789–2809, https://doi.org/10.1175/JAS-D-13-0314.1.

Zawislak, J., and E. J. Zipser, 2014: Analysis of the thermodynamic properties of developing and nondeveloping tropical disturbances using a comprehensive dropsonde dataset. *Mon. Wea. Rev.*, **142**, 1250–1264, https://doi.org/10.1175/MWR-D-13-00253.1.

——, H. Jiang, G. R. Alvey III, E. J. Zipser, R. F. Rogers, J. A. Zhang, and S. N. Stevenson, 2016: Observations of the structure and evolution of Hurricane Edouard (2014) during intensity change. Part I: Relationship between the thermodynamic structure and precipitation. *Mon. Wea. Rev.*, **144**, 3333–3354, https://doi.org/10.1175/MWR-D-16-0018.1.

Zeng, Z., Y. Wang, and L. Chen, 2010: A statistical analysis of vertical shear effect on tropical cyclone intensity change in

the North Atlantic. *Geophys. Res. Lett.*, **37**, L02802, https://doi.org/10.1029/2009GL041788.

Zhang, F., and D. Tao, 2013: Effects of vertical wind shear on the predictability of tropical cyclones. *J. Atmos. Sci.*, **70**, 975–983, https://doi.org/10.1175/JAS-D-12-0133.1.

——, ——, Y. Q. Sun, and J. D. Kepert, 2017: Dynamics and predictability of secondary eyewall formation in sheared tropical cyclones. *J. Adv. Model. Earth Syst.*, **9**, 89–112, https://doi.org/10.1002/2016MS000729.

Zhang, J. A., and R. F. Rogers, 2019: Effects of parameterized boundary layer structure on hurricane rapid intensification in shear. *Mon. Wea. Rev.*, **147**, 853–871, https://doi.org/10.1175/MWR-D-18-0010.1.

——, ——, P. D. Reasor, E. W. Uhlhorn, and F. D. Marks Jr., 2013: Asymmetric hurricane boundary layer structure from dropsonde composites in relation to the environmental vertical wind shear. *Mon. Wea. Rev.*, **141**, 3968–3984, https://doi.org/10.1175/MWR-D-12-00335.1.

——, ——, ——, and J. Gamache, 2023: The mean kinematic structure of the tropical cyclone boundary layer and its relationship to intensity change. *Mon. Wea. Rev.*, **151**, 63–84, https://doi.org/10.1175/MWR-D-21-0335.1.